AD-A055 676 SCIENCE APPLICATIONS INC MCLEAN VA F/G 17/1
ACOUSTIC FLUCTUATION MODELING AND SYSTEM PERFORMANCE ESTIMATION--ETC(U)
JAN 78 R C CAVANAGH N00014-76-C-0753
UNCLASSIFIED SAI-79-738-WA-VOL-2 NL

1 OF 2
ADA
055676

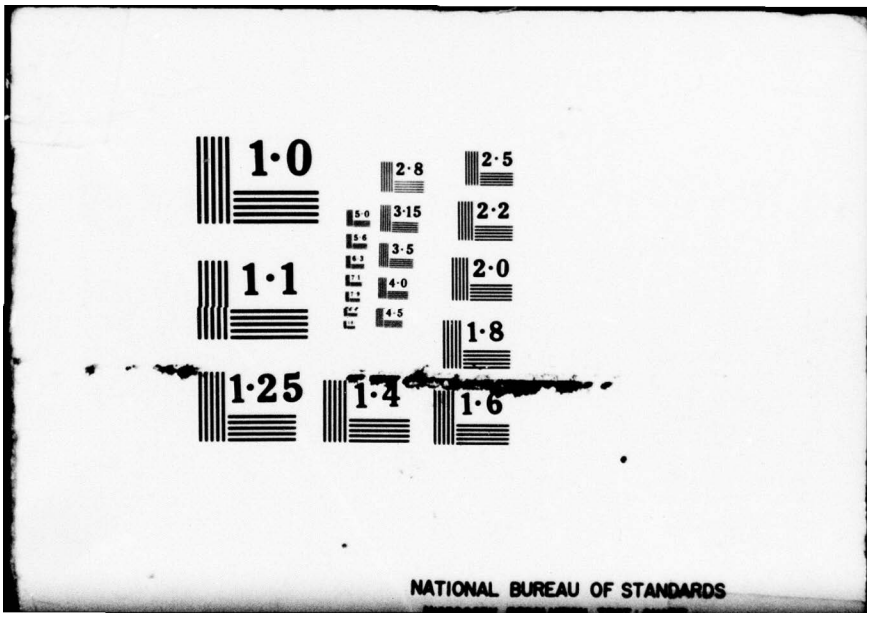
1·0
1·1
1·25
2·8
3·15
3·5
4·0
4·5
5·0
1·4
2·5
2·2
2·0
1·8
1·6
NATIONAL BUREAU OF STANDARDS

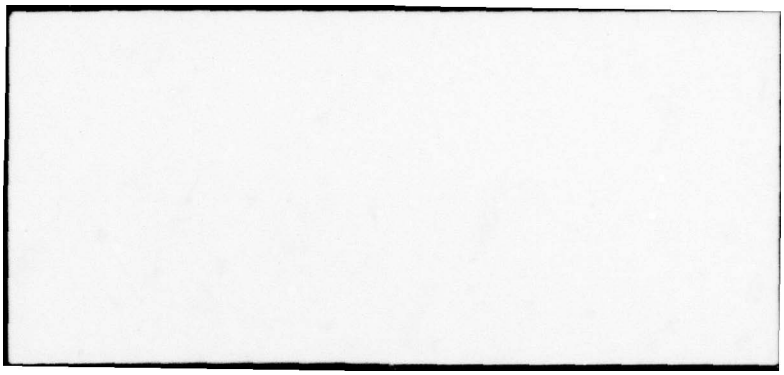

(3)

AD A055676

ACOUSTIC FLUCTUATION MODELING AND SYSTEM PERFORMANCE ESTIMATION

VOLUME II,
APPENDICES

SAI
ATLANTA • ANN ARBOR • BOSTON • CHICAGO • CLEVELAND • DENVER • HUNTSVILLE • LA JOLLA
LITTLE ROCK • LOS ANGELES • SAN FRANCISCO • SANTA BARBARA • TUSCON • WASHINGTON

UNCLASSIFIED

MIL-STD-847A
31 January 1973

SECURITY CLASSIFICATION OF THIS PAGE (When Data Entered)

REPORT DOCUMENTATION PAGE	READ INSTRUCTIONS BEFORE COMPLETING FORM
1. REPORT NUMBER	2. GOVT ACCESSION NO. / 3. RECIPIENT'S CATALOG NUMBER
4. TITLE (and Subtitle) (6) ACOUSTIC FLUCTUATION MODELING AND SYSTEM PERFORMANCE ESTIMATION, VOLUME II, Appendices	5. TYPE OF REPORT & PERIOD COVERED (9) Final rept., / 6. PERFORMING ORG. REPORT NUMBER
7. AUTHOR(s) (10) R. C. Cavanagh	8. CONTRACT OR GRANT NUMBER(s) (15) N00014-76-C-0753
9. PERFORMING ORGANIZATION NAME AND ADDRESS Science Applications, Inc. 8400 Westpark Drive McLean, VA 22101	10. PROGRAM ELEMENT, PROJECT, TASK AREA & WORK UNIT NUMBERS 65152N R0145 NR274-266
11. CONTROLLING OFFICE NAME AND ADDRESS Naval Analysis Program (Code 431) Office of Naval Research Arlington, VA 22217	12. REPORT DATE (11) 4 Jan[illegible]78 / 13. NUMBER OF PAGES 107
14. MONITORING AGENCY NAME & ADDRESS (if different from Controlling Office) (12) 433 p.	15. SECURITY CLASS. (of this report) UNCLASSIFIED / 15a. DECLASSIFICATION/DOWNGRADING SCHEDULE

16. DISTRIBUTION STATEMENT (of this Report)

Approved for Public Release; Distribution Unlimited

(16) R0145 (17) R0145

17. DISTRIBUTION STATEMENT (of the abstract entered in Block 20, if different from Report)

Reproduction in whole or in part is permitted for any purpose of the United States Government.

18. SUPPLEMENTARY NOTES (14) SAI-79-738-WA-VOL-2

19. KEY WORDS (Continue on reverse side if necessary and identify by block number)

SONAR DETECTION
UNDERWATER SOUND TRANSMISSION
UNDERWATER AMBIENT NOISE

20. ABSTRACT (Continue on reverse side if necessary and identify by block number)

This two volume report documents an investigation into several aspects of the validity of the random-process approach. Among the topics considered are:

→ next Page

DD FORM 1 JAN 73 1473 EDITION OF 1 NOV 65 IS OBSOLETE

UNCLASSIFIED

SECURITY CLASSIFICATION OF THIS PAGE (When Data Entered)

408 404 slt

20. ABSTRACT (Continued)

(a) the basic statistical properties of acoustic signal and noise fluctuations

(b) the ability of the random-process models to properly simulate the important properties of the acoustic variables

(c) the ability of the stochastic models to accurately predict measures of system effectiveness

(d) the choice of a stochastic model and estimation of its inputs, for a particular scenario.

Volume II is a compilation of appendices which provide references, calculations, documentation and background information to support the results reported in Volume I.

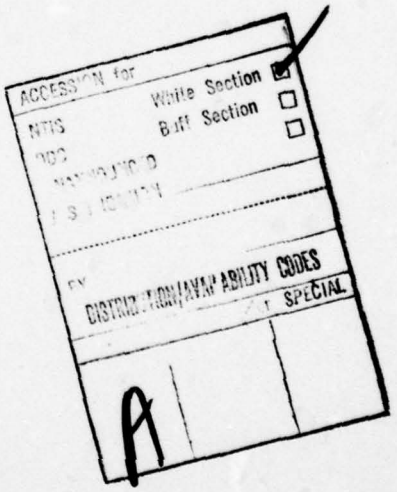

ACOUSTIC FLUCTUATION MODELING AND SYSTEM PERFORMANCE ESTIMATION VOLUME II APPENDICES

Report to

Office of Naval Research
Naval Analysis Program
Attn: James G. Smith, Code 431

January 4, 1978

Final Report
Contract N00014-76-C-0753
Task No. (NR 274-266)

Prepared by:

R. C. Cavanagh

SAI 79-738-WA

SCIENCE APPLICATIONS, INC.
8400 Westpark Drive
McLean, Virginia 22101
Telephone: (703) 821-4300

Executive Summary

This volume consists of Appendices which elaborate on certain topics brought up in the main text of Volume I.

Appendix A provides definitions of statistical properties for stochastic processes and fluctuation data analysis.

Appendix B gives an overview of sonar performance prediction, including the various types of acoustic and system models and levels of simulation.

Appendix C describes the acoustic signal and noise models used in the study, and discusses their validity.

Appendix D surveys statistical fluctuation models based on an acoustic mechanism: varying multipath interference caused by source/receiver motion. The various statistical distributions and correlation functions are shown to be closely related.

Appendix E describes some stochastic fluctuation models which are not derived from properties of the acoustic field but are in common use in performance modeling.

Appendix F discusses the approach used in the study to simulate a sonar signal processor and detector.

Appendix G provides justification for certain results used in the study about array response: the relative importance of transmission-loss and beam-pattern-induced fluctuations, conditions under which beam splitting can be ignored, and the effect of sidelobe suppression on noise fluctuations.

Appendix H documents the algorithms used to model signal and noise and the statistical analysis package.

CONTENTS

CONTENTS (Cont'd)

Introduction

This volume is a compilation of appendices which provide references, calculations, documentation, and background information to support the results reported in Volume I. Most of the material is mentioned or summarized in the main text of Volume I, so that the purpose of this report is to elaborate on the details for the interested reader. Each appendix addresses a single topic, and can be read as a stand-alone document, with its own references and figures.

Appendix A

SOME DEFINITIONS FOR STOCHASTIC PROCESSES AND STATISTICAL PROPERTIES OF FLUCTUATIONS

In Volume I, acoustically modeled time series of signal, noise, and transmission loss are compared with series generated from stochastic processes. The comparison is of statistical properties of the two types of data. In the case of the stochastic process, there are underlying statistical properties which in fact define the process; the time series are simply realizations or samples from the process. The first part of this Appendix sets down definitions of terms commonly used to describe the statistical properties of stochastic processes.

For the acoustically modeled data, basic statistical properties are not usually known in advance, but rather must be determined (estimated) from analysis of the time-series themselves. Moreover the properties of interest in this study are not necessarily the same as those used to define the stochastic processes. Hence, for comparison of the acoustic and stochastic model outputs, specific statistical properties had to be chosen. That choice is the subject of the second part of this Appendix.

A.1 Some Definitions for Stochastic Processes

These definitions of properties of stochastic processes follow the more popular references (A-1 through A-3).

- Stochastic Process. A stochastic process is a family of random variables $\{X(t), t \in T\}$, where T is a set of indices - usually associated with time. In this paper X will be real-valued, and T either a sequence (in which case X is called a discrete parameter process) or an interval (with X a continuous parameter process).

- Sample Function. The function of t obtained by sampling X at each t is a sample function or realization or sample path of the process X.

- Distribution Functions. A stochastic process X(t) is determined statistically by its n^{th} order distribution functions:

$$P[X(t_1) \leq A_1,\ X(t_2) \leq A_2, \ldots, X(t_n) \leq A_n]$$

$$\equiv F(A_1, A_2, \ldots, A_n;\ t_1, t_2, \ldots, t_n),$$

for any n, $\{t_i\}$ and $\{A_i\}$.

The corresponding density function of X(t) is

$$\frac{\partial^n}{\partial A_1 \partial A_2 \ldots \partial A_n} \left[F(A_1, \ldots, A_n;\ t_1, \ldots, t_n)\right]$$

$$\equiv f(A_1, A_2, \ldots, A_n;\ t_1, t_2, \ldots, t_n).$$

- Expected Value. For t fixed $E[X(t)] = \int z f(z;t)dz$ is the expected value or ensemble average of X at t.

- Autocovariance. $C(t_1,t_2) = E\{[X(t_1)-\mu(t_1)]\cdot[X(t_2)-(t_2)]\}$ where $\mu(t_i) = E[X(t_i)]$

- Autocorrelation. $R(t_1,t_2) = E[X(t_1)X(t_2)]$

  Note that $C(t_1,t_2) = R(t_1,t_2) - \mu(t_1)\mu(t_2)$ and $E[X(t)]^2 = C(t,t) = R(t,t) - [\mu(t)]^2$.

- Stationary Process. X(t) is stationary in the strict sense if its joint distributions do not change with t, i.e.,

  $$F(A_1,A_2,\ldots,A_n;t_1+h,t_2+h,\ldots,t_n+h)$$
  $$= F(A_1,A_2,\ldots,A_n;t_1,t_2,\ldots,t_n) \text{ for any } h$$
  with t_i+h in T.

  X(t) is stationary in the wide sense if

  $$E[X(t+h)X(t)] = R(t+h,t) \equiv R(h) \text{ for all } t,$$

  and $E[X(t)] = \mu$ is independent of t.

- Ergodicity. Let X(t) be stationary and defined for all real t. If the time-average of X,

$$\langle X(t) \rangle = \lim_{T \to \infty} \frac{1}{2T} \int_{-T}^{T} X(s)ds,$$

exists and equals the constant $E[X(t)]$ with probability 1, then X is said to be <u>ergodic in the mean</u>.

Now, X(t) is <u>ergodic</u> if (with probability 1) all its statistics can be determined from a single sample function from X.

A sufficient condition (Birkhoff-Khintchine, see Ref. A-4) for a stationary, continuous process to be ergodic is that it have finite variance and an autocovariance function which converges to zero as the lag tends to infinity.

A stationary Gaussian random process with zero mean is ergodic if

$$\int_{-\infty}^{\infty} |R(\tau)| d\tau < \infty.$$

- <u>Power Spectral Density</u>. For a wide-sense stationary process X(t), the <u>power spectral density</u> or <u>power spectrum</u> at angular frequency ω is

$$S(\omega) = \int_{-\infty}^{\infty} R(\tau) e^{i\omega\tau} d\tau.$$

If $X(t)$ is also ergodic and $S(\omega)$ exists, then

$$S(\omega) = \lim_{T\to\infty} \frac{1}{2T}\left|\int_{-T}^{T} X(t)e^{i\omega t}dt\right|^2$$

with probability one.

The power in band Ω is $\frac{1}{2\pi}\int_{\Omega} S(\omega)d\omega$.

- Markov Process. $X(t)$ is a Markov process if for every n and $t_1 < t_2 < \ldots < t_n$,

$$P[X(t_n) \leq A | X(t_{n-1}),\ldots,X(t_1)]$$

$$= P[X(t_n) \leq A | X(t_{n-1})]$$

or equivalently

$$P[X(t_n) \leq A | X(t) \text{ for all } t \leq t_{n-1}]$$

$$= P[X(t_n) \leq A | X(t_{n-1})].$$

- Gaussian Process. $X(t)$ is a Gaussian or normal random process if the random variables $X(t_1)$, $X(t_2)$,..., $X(t_n)$ are jointly normal for any n and $\{t_i\}$.

A.2 Statistical Measures for Comparison

The primary purpose of the comparisons of acoustically and stochastically modeled time series is not to test the hypothesis that two series are sample functions from some common, underlying process but rather to determine if the two series possess the same detection-related properties. Accordingly, a number of statistical descriptors have been selected for their relevance to sonar performance, and it is in terms of these properties that the comparisons are presented.

It is emphasized that the "validity" of a particular model depends on the application. The properties chosen here are believed to be broad enough to allow a user to judge whether or not a simulation enjoys the accuracy required for his particular case.

A.2.1 One-Dimensional Distribution Functions and Moments

The statistical package described in Appendix H was applied to both acoustic and stochastic fluctuation time series to determine:

- one-dimensional sample distributions
- corresponding moments (mean, variance, skewness, kurtosis)
- percentiles and the range of the data

In accordance with the discussion of Appendix D about candidate distribution functions for fluctuations of

TL and noise intensity, the sample distribution functions were subjected to the two-sided Kolmogorov test for fit against the logarithmic transform of the:

- log-normal distribution
- chi-square distribution (exponential and gamma), arbitrary number of degrees of freedom (d.f.)
- non-central chi-square distribution with 2 d.f. and arbitrary noncentrality parameter.

In each case "best" parameters were selected by matching the distributions at the median (using the arbitrary location parameter), fitting the candidate distribution to the sample distribution at the 15th and/or 85th percentiles (using scale or shape parameters), and then testing. The test was also repeated with the median shifted in steps up to 1.5 dB, allowing for the possibility that the match of medians was not proper.

The Kolmogorov statistic is the largest difference (D_n) between the candidate and sample distribution functions, the latter based on n independent samples. The test then derives from the probability:

$$P[D_n > C(n,\alpha)] = \alpha$$

where $C(n,\alpha)$ is obtained from tables and α is called the significance level, usually taken to be 0.01 or 0.05. If the Kolmogorov statistic D_n satisfies

$$D_n < C(n,\alpha),$$

then the hypothesis that the samples were drawn from the candidate distribution is not rejected at the significance level α, i.e., the size of D_n is consistent with what would be expected with probability $1-\alpha$ (the "confidence level"):

$$P(D_n < C) = 1-\alpha.$$

One complication with the application of the Kolmogorov test is in determining the number n of independent samples, since $C(n,\alpha)$ is asymptotic to $1/\sqrt{n}$ and the test is thus quite sensitive to the value of n. In the results given below, two time-series samples are treated as independent if they are separated in time by an amount for which the autocovariance function is small. Of course, zero correlation implies independence only under very special conditions, but a conservative test results when n is calculated in this way.

A.2.2 Autocorrelation Properties

In determining the temporal properties of the data, this investigation stopped short of calculating sampled joint-density functions and concentrated on the temporal autocovariance function and its Fourier transform (Power Spectral Density). The former is important in current stochastic modeling, while the latter displays the underlying periodicities of the time series. In interpreting the results, note that an assumption of ergodicity (and hence also stationarity) has been imposed - since time (and not ensemble) averaging is performed and correlation is calculated as a function of time lag only.

The Fourier transform is called a "spectrum" in this report, but it is not the conventional power spectral density of pressure. In fact, the autocovariance is for the log transform of intensity and thus the spectrum defies interpretation as anything more than an identification of the oscillation periods of the dB variable. Moreover an FFT has been employed and the discrete spectrum values are to be viewed as averages over "frequency" bins of size approximately equal to the reciprocal of the maximum lag time of the autocovariance function (which lag is in turn about 25% of the duration of the time series).

A.2.3 Stationarity and Ergodicity

A "conventional" test for stationarity has been applied to the time series: it simply calculates moments over subintervals of time. Since the sample time series are always of finite duration, a non-stationary series and a stationary one with a low-frequency trend cannot be distinguished. In fact, the stochastic process models which are constructed as stationary processes can show radically different moments from interval to interval (the results of Volume I show examples). For calculation of time-series statistics, this study in essence assumes that all processes are stationary, but with long-term trends which cannot be quantified because of the short sample times.

Most of the statistical calculations also implicitly assume ergodicity by using time averages in place of ensemble averages. However, in cases for which there are many replications (e.g., ambient-noise acoustic simulations), both types of averages are found and a comparison made. In fact, in one case for which the time duration of the series was too

short (compared with the decorrelation time) to yield many uncorrelated samples, the ensemble statistics were used as a more reliable estimate of moments. A Smirnov test for equivalence of distribution functions from two different time-series replications was also performed.

A.2.4 Cross-Correlation Properties

In only two cases was the cross-correlation of two time series investigated. First, for a few replications of acoustically modeled noise, the normalized cross-covariance was found to be uniformly small, and all replications were treated as independent. Secondly, acoustically modeled beam noise samples from two different beams but from the same replication of the noise field were cross-correlated. The results varied from sample to sample, from high to low to negative correlation, indicating that further study is needed before trends can be predicted.

A.2.5 Level-Crossing Properties

Among the most important statistical properties of the time series are the intervals of time for which the data are above or below a threshold level - this is the essence of the detection application. Accordingly, time series of TL, noise and signal excess were input to a "detector" package (described in Appendix H) which determined for a given level L:

(i) Time to first and last passage above (below) L,

(ii) Sample distribution of time intervals for which the series is above (or below) L,

(iii) Sample probability that a time interval of length s contains at least one point above (or below) L,

(iv) Sample distribution and moments of waiting time to passage above (or below) L,

(v) Sample distribution and moments of waiting time to "sustained" passage above (or below) L.

The first of these is of little value without much replication, while the second is fundamental to most of the others and yields "detection probability" and "holding times." "Cumulative detection probability" is the motive for (iii), calculated as the fraction of intervals of length s with at least one point above L, or directly from (ii) as one minus the fraction of intervals of length s with no points above L.

The distribution of waiting times (iv) can be found from (ii) as

Sample Probability that the Waiting Time is Zero

≡ Sample P(Waiting Time = 0)

= fraction of points above L,

and

Sample P(Waiting Time = T)

= (Number of intervals of length T or more with all points below L)/Total number of points

Finding the distribution of modified waiting time (v) is more complicated and requires estimation of the probability of waiting for a time period M until the time series has remained above the level L for period K. The sample estimate for $M \leq K$ is

Sample P(Waiting Time = M)

= (Number of intervals of length K or more with all points above L)/Total number of points

while for $\tau \geq 1$,

Sample P(Waiting Time = $K + \tau$)

= (Number of intervals of length τ or more in the complement of the set of all intervals of length K or more)/Number of points

For the comparisons of Volume I the focus is on (ii) - (iv). The modified waiting times (v) can certainly be important, but the scope of the present study was limited.

REFERENCES

A-1 Doob, J. L., Stochastic Processes, Wiley, New York (1953)

A-2 Papoulis, A., Probability, Random Variables, and Stochastic Processes, McGraw-Hill, New York (1965)

A-3 Parzen, E., Stochastic Processes, Holden-Day, San Francisco (1962)

A-4 Gnedenko, B. V., The Theory of Probability, Chelsea, New York (1962)

Appendix B
OVERVIEW OF SONAR PERFORMANCE PREDICTION

The primary objective of this study is to determine how the modeling of the acoustic environment affects the prediction of sonar-system performance. The investigation has been performed for a very special case (a single ocean environment, a generic towed-array system, a special detector, a limited number of target tracks, a stable source, etc.). Throughout the report of results (Volume I) are references to various kinds of models: environmental, acoustic, performance, engagement, sonar-equation; and to model outputs: ambient noise levels, signal time series, measures of effectiveness (MOE's), detection probabilities, etc. This Appendix presents an overview of the various model types and applications. The purpose is to show how the specifics of this study relate to the general performance-prediction problem.

B.1 Acoustic and Performance Prediction

Consider first that "predictive capability" is what is sought here, i.e., the capability to estimate in advance characteristics of the system performance or engagement results. In that case, the reconstruction of exercise results, the explanation of time-series data, or the understanding of the dominant mechanisms can be viewed as development or evaluation of the "predictive capability." The word "model" is then used in a general sense to describe method of prediction: it can be based on an understanding of the first principles underlying the physical phenomena, or it can be a strictly empirical, parameterized fit to measured data. Empirical models require a substantial

quantity of supporting data, and cannot be applied with confidence outside the regime of the measurements. Models based on first principles generally require less measured data and can be extrapolated with some degree of confidence.

There is then a hierarchical ordering of models relevant to sonar system analyses:

- Environmental Acoustic Models

  These estimate properties of signal propagation and noise for given locations, geometries, times, frequencies, etc., and provide inputs to performance models. Implicit in the definition of this class of models are the environmental models which provide the inputs, e.g., sound speed, wave spectrum, bathymetry, bottom reflectivity, etc. Acoustic models may be deterministic or random, and may be required to predict the actual value of a variable for specified conditions or a statistical characterization over an ensemble of conditions. A good example is that of ambient noise for arrays; depending on the application, the noise model might be called upon to predict such things as:

  - plane-wave intensities as a function of angle, averaged over a large ocean area and over a season

  - statistics of temporal fluctuations of plane-wave intensities, at a specified location and over a short time interval

- statistics of the cross-spectral density of noise power for pairs of hydrophone locations, ensembled over a number of surface ship traffic patterns.

- Sonar Performance Models

  These models combine the acoustic data with the target and sonar-system properties to yield estimates of sonar-system performance. In most cases, the model must estimate a measure of effectiveness (MOE) under specified conditions about location, target/sonar geometry, sonar platform conditions, etc. It then must simulate the response of the sonar system to a given target. Again, this type of model may treat variables as deterministic or random, and may yield ensembled statistics or single estimates of the MOE.

  In the example of a towed array, the model might be called upon to predict the range at which a particular target in a specified acoustic environment will be detected. The results may then have to be ensembled statistically over time or location or target velocities or whatever.

  Examples of performance models are SHARPS, TASSRAP, SIMAS, OMS, PEP Level II, PASS.

- Engagement Models

  The engagement models go beyond sonar performance to predict MOE's related to more

complicated Naval engagements - including such activities as weapon delivery, tactics, or follow-up processes. In so doing, they must use performance models for one or more sonars, for weapons, for platforms, etc.

Examples of engagement models are APAIR, APSUB, SIM II, PEP.

The present study concentrates on the characterization of fluctuations for certain acoustic and performance models, but stops short of an investigation of the engagement models.

B.2 Application and Validation of Models

B.2.1 Environmental Acoustic

Environmental acoustic models have as their primary application the use in performance models to predict sonar effectiveness. Other applications, such as interpretation of acoustic data, are in the realm of evaluation or improvement of the acoustic models themselves.

For acoustic models based on physics principles, evaluation is carried out extensively by the R&D community via carefully controlled scientific experiments in which the mechanisms hypothesized as dominant are closely monitored. It is nearly impossible to "validate" a transmission loss model if the source/receiver geometries and ocean environmental conditions are not known. Empirical models are considered valid for the conditions corresponding to the data on which they are based (if known) and nowhere else. Rules

of extrapolation are usually based on physical principles and so convert the empirical model to a physical model. Appendix C discusses the validation of the particular acoustic models used in this study.

B.2.2 Performance

Performance models have a broad spectrum of applications, including:

- concept evaluation
- design of systems
- trade-off of system candidates
- deployment optimization
- cost-effectiveness and force level analyses
- optimization of system operation and tactics
- engagement reconstruction
- exercise planning

Each has its own requirements for MOE accuracy, ensembling, etc.

Evaluation of performance models is a controversial subject, and should be viewed in terms of the objective (presumably a predictive capability) and the type of model (empirical or based on first principles). First, a model based on physical principles must consist of components accounting for the target characteristics, the acoustic environment, the source/receiver geometries, the sonar system response to the signal and noise, and the detection process

(manual or automatic, including classification or localization). If the quantitative importance of each component is determined and if each component is found to have the appropriate accuracy, then there is a basis for "validating" the performance model as a predictive capability. On the other hand, if the sonar system behavior is nontrivially dependent on the component variables and if the components cannot be evaluated, then the number of unknowns will usually preclude "validation" of the performance model unless enormous quantities of performance data are available. Needless to say, empirical performance models demand even more data for evaluation.

B.3 Basis and Output of Performance Models

The outputs of performance models are quantitative predictions of system performance, usually called measures of effectiveness (MOE's). Examples of interest to the surveillance and tactical sonar community are:

- Area Coverage
- Detection Contours
- Sweep Rate
- SPA Size
- Instantaneous Detection Probability
- Cumulative Detection Probability
- Distribution of Holding-Time Intervals
- Time to Lost Contact
- Time to Reacquire

- Time to Classify or Localize
- Barrier Effectiveness

Each has a definition complicated by the ensemble of conditions over which the estimates are to apply. To focus this study, it is proposed that detection histories, or at least detection-probability histories, are the underlying variables for most of these MOE's.

Given that detection history is the principal output and that the target and environmental parameters are the inputs, the basis for the performance model is nothing more than a sonar equation, which itself should be viewed as a model. It gives the system detection characteristics as a function of input signal and noise properties. In general, the sonar equation relevant to performance modeling is of the form:

$$S = SL - TL + ASG + PGS$$

$$N = AN + ANG + PGN$$

where all quantities represent relative intensities (mean-square pressures) in dB's, and

S = signal level, after processing,

SL = source level,

TL = transmission loss from source to receiver,

ASG = array gain for the signal,

PGS = processing gain for the signal (including operator),

N = noise level, after processing,

AN = all noise before processing,

ANG = array gain for noise,

PGN = processing gain for noise.

The signal-plus-noise is the phased sum of S and N. Each variable can be viewed as time-varying or constant, as a random variable or as deterministic. The performance model first estimates such quantities and then determines appropriate detection histories based on the system's detection algorithm.

As discussed in Appendix F, most performance models relevant to low-frequency, passive systems have as detection algorithm the thresholding of signal-to-noise ratio (SNR). In terms given above, a detection is called if

$$f(S-N) > TH$$

where TH is the threshold and f is a functional operating on S-N (the SNR). Now, TH may be time-dependent (e.g., allows for alerting) and may have to be treated as a random variable since it embodies operator performance. The function, f, may represent scaling, squaring, time-integration, etc. The "usual" sonar equation and the one used in this study is found for f the identity operator and

$$S - N = TL - TL - AN + (ASG - ANG) + (PGS - PGN)$$

$$\equiv SL - TL - AN + AG + PG$$

where AG is total array gain and PG is processing gain. Then

$$P_D = \text{Probability of Detection} = P(S\text{-}N > TH).$$

If "signal excess" is defined as

$$SE = (S - N) - TH,$$

then detection occurs whenever $SE > 0$. Hence, in this case, the performance model can provide either detection histories via a time series of SE (and perhaps TH) or detection probabilities via $P(SE > 0)$.

Appendix C
THE ACOUSTIC MODELS AND THEIR VALIDITY

Transmission loss and noise predictions generated frcm state-of-the-art acoustic models serve as the control data for this study. They provide deterministic, known acoustic environments which serve as "real data" for the test of selected stochastic models and also assist in explaining fluctuation mechanisms and developing improved stochastic simulations. In what follows, the rationale for the use of acoustic models instead of measured data and the assumptions/limitations associated with such an approach are discussed. In addition, some details about the particular models and their validity are presented.

C.1 Acoustic Fluctuation Mechanisms

At low frequencies in a deep water environment, the signal level received by an omni-directional hydrophone from a moving narrowband source fluctuates in time. Long-term variations in average received level might be associated with the source moving through convergence zones. Superimposed on this envelope is a rapid variation caused by the changing phases of the various propagation paths connecting the source and receiver. Under many circumstances, these phase fluctuations have been shown to be the results of changes in range. In other words, the detailed variations observed in time series of received signal level are due simply to the source moving the complicated multipath interference patterns of the

acoustic field past the receiver. While the precise positions of peaks and nulls in the transmission-loss fluctuations are not predictable, there are convincing demonstrations that the distributions of received levels, as well as the spatial (range) spectra of transmission loss, can be accurately estimated using propagation models which combine all paths on a fully-coherent basis. Hence, for a particular range of CPA and target speed, a representative time series of received signal level can be generated. Since, at low frequencies, the ambient-noise field consists of contributions from surface ships, it follows that the ambient-noise variability can be simulated by combining the received signals from all relevant surface ships. Finally, fluctuations in the output of beamed systems can be simulated by taking into account the array response to the signal and noise fields.

Although it is assumed to be the case for this study, the dominance of motion-related, multipath fluctuations for TL is not universal. When relative source/receiver speeds are low, the effects of the dynamic ocean medium (fronts, internal waves) may contribute significantly to the total TL fluctuation.

C.2 Signal Fluctuation Modeling

Signal fluctuations are simulated by tracking sources through the multipath interference patterns in the acoustic field modeled by either ray or wave propagation codes. The resulting time series can be scaled, shifted, averaged, and combined with array response

patterns to simulate a number of target speeds and bearings from the array. The incoherent averaging appropriate to the signal processor can be applied to these time series via the detector simulation.

The transmission loss simulations used in this study are derived from the Parabolic Equation (PE) model (Ref. C-1) for RR and RSR paths and from a version of the FACT model (Ref. C-2) for bottom bounce propagation. A combination of the two models is considered to be the best available method for simulating the fluctuations of the transmission loss for the case at hand. The PE technique is an extremely accurate and efficient approach for refracted paths, but is presently unable to properly handle the high-loss bottom bounce paths. Hence, output of the FACT model for the coherently-summed bottom-bounce multipaths is added in phase to the refracted-path field generated by PE. This FACT contribution is important only to ranges of about 100 nm.

The TL model output is transmission loss as a function of range, TL(R), for a narrowband signal at 25 Hz. It is sampled every 1/6 nm and exhibits the multipath interference in full detail. Given the target source level SL(t) and range rate R(t), the time series of the signal is found from:

$$S(t) = SL(t) - TL[R(t)].$$

Note that for a given target and ocean environment the signal model is completely deterministic; fluctuations arise solely from source motion through the multipath interference field. There is no attempt to account for fluctuations due to the variations in the medium with similar time scales, nor are the range/azimuth-dependencies in the environment treated in detail. In fact, if a stable source is at constant range from the receiver, whether moving or not, this model will yield a signal which is constant in time (except, perhaps, for modulation by the beam pattern).

C.2.1 Model Validity

First of all, the environmental inputs (sound speed, bottom reflectivity, bathymetry) correspond to a PARKA II-A Experiment track (Ref. C-3).

FACT is the Navy Interim Standard transmission loss model for range-independent environments. It has been subjected to extensive comparisons with data - especially for the PARKA conditions-and has been shown to give very reliable results whenever the environmental inputs are accurate. For the case under consideration, the environment is effectively treated as range-independent to ranges of about 100 nm, where the bottom bounce energy becomes negligible.

Although not yet a Navy Standard, the PE model has also been evaluated against a number of measured data sets. Of particular relevance is the comparison of Ref. C-4 with PARKA II-A shot data. Typical distributions of

the difference between measured and predicted transmission loss at low frequency show means less than 1 dB and standard deviations on the order of 2 dB.

In view of the agreement of the transmission loss model with measured data for the test environment of this study (viz., to the limit of measurement accuracy), it is easy to argue for the use of model predictions instead of the measured data: the model extrapolates to other source/receiver geometries, ranges, frequencies, and even environments, and in fact can show sensitivities to these parameters.

C.3 Noise Fluctuation Modeling

Ambient noise can be simulated under the assumption that at low frequencies there are two basic components:

(i) a steady background associated with very distant ships and wind action on the sea surface, and

(ii) a fluctuating component associated with nearby surface ships as they move through the multi-path interference patterns and convergence zones.

Given the set of surface ships in the basin of interest, their radiated noise and velocities, a set of "signals" can be calculated deterministically with the aid of the detailed transmission loss function, just as in the case

of the target signal. These contributions from individual ships can then be summed at the receiver to yield the time series of ship-generated noise. Its fluctuations are again driven by the multipath interference and convergence zone properties of the transmission loss - but complicated by the fact that several (or many) sources are present.

For the present study, the surface-ship contributions are calculated with the DSBN Model (Appendix H), in the same way as for signal. The i-th ship with source level $SL_i(t)$ and range rate $R_i(t)$ generates a signal,

$$S_i(t) = SL_i(t) - TL[R_i(t)],$$

and the collective signals make up the noise field.

As described in Appendix H, the model uses a hypothesized set of surface ships, moving on straight-line courses across the basin and radiating noise correlated with their speeds. If the ship source levels and courses were known, the model would be completely deterministic; but since they are not, these parameters are treated as random variables subject to constraints imposed by somewhat general bounds (e.g., speeds are 15 knots ±5 knots, courses are within 15° of 90° or 180°T. source levels are near 163 dB but depend on a random length and on speed, ship densities on average over time must be consistent with those observed). For each point in time, the radiated noise from each ship propagates to the receiving array. The resultant contributions are added incoherently (random phase), under the assumption that fluctuations associated with a coherent sum are

typically averaged out by the signal precessor's time integration. Transmission loss is derived from the modified PE model described above, with a source depth of 60 feet, and is corrected to simulate loss from a near-surface source which radiates only away from the surface. The simulated noise time series is sampled every two minutes for the duration of a replication (e.g., 10 hours). Each replication is initialized by random selection of ships, speeds, courses and source levels.

C.3.1 Model Validity

Questions can be raised about several of the assumptions inherent in this model:

(a) How representative are the source levels?

(b) Is the mechanism for coupling the radiated noise to the propagation paths treated realistically?

(c) Is the envelope of the radiated noise from a single ship as observed in a narrow band properly treated as constant?

(d) Should the radiated noise be aspect-dependent?

(e) Are important fluctuation properties lost when the noise components from different ships are added incoherently at the receiver?

(f) Are important fluctuation mechanisms overlooked when transmission loss is modeled as independent of bearing?

For (a) through (d), estimates of the radiated noise properties are the best available but of questionable accuracy. There are several Navy R&D projects in progress now to measure and model merchant/fishing ship sources. For the present study, the most important of the first four is (c), but there is no substantive evidence to suggest that two-minute averages are not stable levels (i.e., the time-bandwidth products are large).

For question (e), it is the time-dependence of the fluctuation process, rather than the marginal distributions, which could be inaccurately simulated as a result of the incoherent summation. It is argued, however, that the interference would be important only if the noise components from two or more ships were of about the same magnitude, the resulting intensity dominated the noise, and the modulation showed significant energy for periods above the sampling rate (here, two minutes). These conditions could certainly occur, but probably not very often or consistently for the array problem treated here. It can be viewed as a secondary effect which warrants future study. Finally, the accurate prediction of absolute noise levels requires a commensurate accuracy in the transmission loss. For the simulation of fluctuations in the environment of this study, it is judged that the multipath characteristics will be similar in all directions and that the use of a single detailed loss function is appropriate.

In spite of the potential inaccuracies from the above or other model inadequacies, we are encouraged by the results of the evaluations of a number of models which are no more sophisticated than the DSBN model. For the prediction of broadband (say, 1/3 octave), averaged (say, more than several hours) noise levels, models which use static ship densities have shown good agreement with data when the environmental inputs were accurate and conditions did not press model limitations; see, e.g., Ref. C-5.

We know of no ambient noise measurement data appropriate for conclusive validation of a model which predicts the detailed time dependence of beam noise, i.e., there are no data with sufficiently accurate information about the environment and sources. There are, however, measurements which are particularly applicable to our study. The NRL SIAM model (Ref. C-6), which is quite similar to DSBN, predicted beam noise statistics from Monte Carlo simulations based on historical shipping densities. The results (Ref. C-7) show reasonable agreement between the measured and predicted distributions of beam noise at 50 Hz.

As a final consideration on the validity of noise simulations, compare the significant confidence associated with a signal prediction against that of a noise prediction suffering from the uncertainties in ship locations, velocities and mean source levels. For a fixed ocean environment and target parameters, the signal simulation can be interpreted as a good approximation to what might be measured; and such model evaluations have been successful in the past. However, in the case

of noise, the detailed ship data for a "deterministic" prediction are not (and never have been) available. Thus, the model is run for shipping fields consistent with the best information available - usually ship densities and percentages by type within grossly-defined lanes.

The rationale then is that a "representative" noise time series generated by a model of this type is the most realistic approximation to true noise data available, and it can be analyzed to determine the dominant mechanisms and the sensitivities to the environment. Since the shipping parameters are so poorly defined, a number of realizations of noise time series are generated from a constrained population of shipping fields - then common statistical properties and a base for predicting them can be identified.

C.4 Signal-Plus-Noise and Signal-to-Noise Ratio Modeling

As noted in Appendix F, there are valid reasons for modeling the detection process as one which thresholds on a function of signal-to-noise ratio (SNR), rather than one which compares the measurable quantities: signal-plus-noise (S + N) and an estimate of noise.

Simulating the latter in its precise sense involves coherent summation of the signal and noise time series as well as modeling the noise estimate - be it in neighboring frequency bins or azimuthal angles. These operations present new problems since they require simulation of the relative phases of signal and noise and of

the "coherence" of noise in frequency or azimuth. Only the last of these is predicted with any confidence by the deterministic models.

In this study, S and N are modeled separately and N is treated as an estimate of noise in a neighboring bin or beam. Thus the problem is avoided. However, a number of assumptions about the signal-processor algorithm and the properties of S, N and S + N have been made in order to justify the SNR detector.

C.5 Array Response Modeling

The complete treatment of a multi-element array requires the fully-phased pressure for both signal and noise at each hydrophone location as a function of time. Array beam outputs can then be simulated by weighting and phase-delay summing these hydrophone outputs. Such a simulation is beyond the scope of the present study, but has been accomplished recently. For the specific type of array used here, a simpler approach is appropriate.

First, suppose that the array is a conventional horizontal line and is not too long, i.e. that it is operating at design frequency, uses weighted delay and sum beamforming, and is no more than about 25 wavelengths long. Then DI is about 17 dB and beamwidths are no smaller than about 4°. Suppose further that the array is straight, stationary, and precisely horizontal. It is not unrealistic then to model waterborne transmission with plane waves which enjoy perfect horizontal coherence (there is some experimental evidence to support this assumption).

If it is assumed that multipath interference arrivals from off-steering-angle sources, across the array length, were within the coherent integration time of the processor, then the array response function could be convolved in both azimuth and elevation with the acoustic signal and noise fields. Since that approach requires the detailed angular arrival structure from every noise source, a further simplification is sought.

It is the detailed vertical structure which is difficult to treat without extensive computer effort, but for a moderate to high-loss bottom, the influence of the vertical arrival structure can be safely neglected for all but near-endfire beams. Hence, in this study, the array beam pattern has been idealized to its response in the horizontal plane, and beams correspondingly near broadside are considered. Additionally, the combinations of beamwidth and level of sidelobe rejection have been constrained so that the sidelobes can be categorized in terms of an average response rather than the detailed structure.

Appendix H describes the computer algorithms for the array-response model.

C.6 Time Scales and Units for Modeled Quantities

It was shown in Appendix F that modeling a narrowband signal detector via thresholding on SNR is reasonable under special conditions related to the processing of the signal-plus-noise and noise. It is important then to state the scales and units of the predictions of signal and noise - so that the interpretation

of detector performance is accurate. It seems that this step is seldom taken in the analysis of performance/engagement models.

The transmission loss prediction (TL(R)) is made in range steps chosen so that smooth interpolation between points is accurate. Each point is best interpreted as the (relative) intensity of the field in a narrow frequency band centered on 25 Hz. For fixed source/receiver geometry the coherent integration time for viewing the narrowband intensity would be several seconds to minutes, while for a moving source there is an additional range average over distances up to 1/6 nm. Since the source is assumed to be stable over many minutes and since the TL varies smoothly over ranges on order of 1/6 nm or more and time periods up to minutes, the incoherently averaged signal over these time (range) scales is about the same as any coherent integration. The rule of thumb then is that the signal intensity prediction for a 5 knot (radial speed) source represents the output of a narrowband (coherent) filter followed by an incoherent integration with total integration time of 2 minutes or less (the 5 knot target covers 1/6 nm in 2 minutes).

The noise model incoherently sums contributions from stable sources moving at speeds from 0 to 20 knots, provides outputs every 2 minutes, and incorporates TL with the scales given above. Hence, the noise estimate must be viewed as the incoherent average of many coherently-filtered samples over 2 minutes. The coherent integration

time may be as long as about 10 seconds, so that there are 12 or more such samples to be averaged.

Because of the constraints imposed on the array and environment given in C.5, the effects of the array response function do not alter this interpretation of signal and noise predictions.

In summary, predicted signal and noise time series samples, taken every 2 minutes, should be interpreted as output of a signal processor which coherently integrates for intervals of time up to 10 seconds and then incoherently averages the results for 2 minutes.

C.7 Acoustic Modeling of Averaged Signal and Noise

The preceding subsections have been concerned with the acoustic modeling of the detailed time series of signal and noise, including the dominant fluctuations. Consider here the prediction of the mean values, about which the variables fluctuate.

It is customary in performance and engagement simulations (Appendix E) to measure or model the "deterministic" part of signal and noise, and then to add to it a "random" part which accounts for what are usually believed to be "random" fluctuations. Figure C-1 shows a detailed TL range series and two smoothed versions typical of what might be used in performance analysis. They are quite different and lead to one of the questions addressed in this study: what <u>are</u> appropriate algorithms

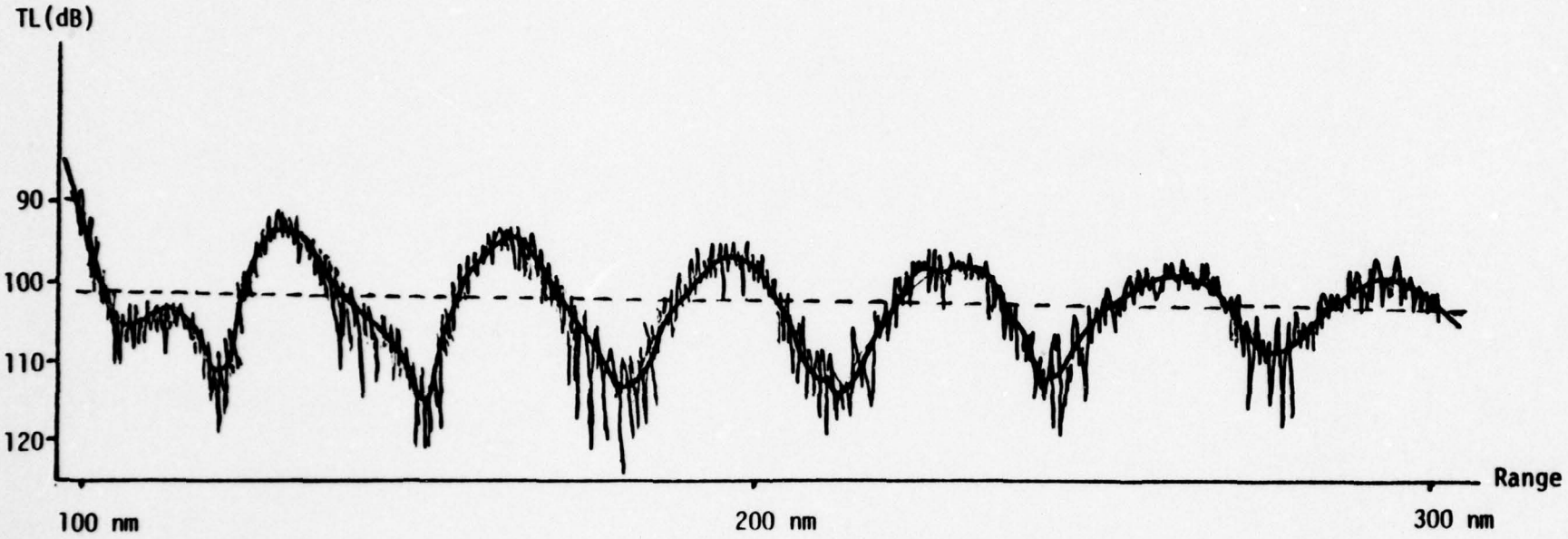

—— 2 nm Intensity Average
---- A+BlogR Fit Over 500 nm

Detailed Transmission Loss and Averages

Figure C-1

for smoothing TL to obtain the "deterministic part," and how do the resulting fluctuation properties depend on them?

Consider first the two extremes: (a) the deterministic part is the mean for the entire time series (or range series of TL), and (b) the deterministic part is the full series, with as much detail as is available from model or measurement. Now, (a) assumes complete ignorance about estimating the locations of peaks and nulls - leaving it to the random process model to yield representative realizations. In (b) it is claimed that the detailed locations and levels of peaks and nulls are realistic and in fact would agree well with measured data if the inputs were known with appropriate accuracy.

The point of view taken here is that (b) is usually the case, but that acoustic prediction capability is often input-limited, especially for noise. Even under input-limited conditions, models can be used to identify common properties over the range of uncertain inputs, as has been done for noise predictions (over shipping) and transmission loss (over range). When these common properties consist of a mean trend plus the distribution and spectrum (and perhaps other properties) of the residual, then a random process model for the fluctuations may be appropriate for mathematical convenience or economy.

For the practical matter of predicting "mean" TL and noise for inputs to performance models, various smoothing algorithms are compared for the test case presented in Volume I. For TL, range averages go from fractions of a mile to an A + BlogR fit, while for noise the detailed data and a mean over the whole series are tested.

REFERENCES

C-1 Hardin, R. H. and F. D. Tappert, SIAM Rev. (Chronicles) 15, 423 (1973); F. D. Tappert and R. H. Hardin, Proceedings of the Eighth International Congress on Acoustics (Goldcrest, London, 1974), Vol. II, p. 452.

Tappert, F. D. and R. H. Hardin, in "A Synopsis of the AESD Workshop on Acoustic Modeling by Non-Ray Techniques, 22-25 May 1973, Washington, D.C.," AESD TN-73-05, ONR, Arlington, VA (Novemeber 1973).

Brock, H. K., "The AESD Parabolic Equation Model," AESD TN-75-07, ONR, Arlington, Virginia (December 1975).

C-2 Spofford, C. W., "The FACT Model (Vol. I)," Maury Center Report 109, ONR, Arlington, VA (1974).

Baker, C. L. and Spofford, C. W., "The FACT Model (Vol. II)," AESD Tech Note TN-74-04; ONR; Arlington, VA (December 1974).

C-3 "PARKA IIA - The Acoustic Measurements - Volume I," Maury Center Report 006, August 1971.

C-4 Hanna, J. S. and P. V. Rost, "An Analysis of PARKA IIA Data Using the AESD Parabolic Equation Model," AESD Tech Note TN-75-09, ONR, December 1975.

C-5 Wagstaff, R. A., "An Ambient Noise Model for the Northeast Pacific Ocean Basin," JUA(USN), July (1977)

C-6 Marshall, S. W., "Acoustic Signal-to-Noise and Azimuthal Noise Directionality in the Mediterranean Sea Using LAMBDA II," NRL Memo 3050, April 1975.

C-7 Marshall, S. W., "Acoustic Performance of LAMBDA II in the Church Opal Experiment," NRL Report Draft, October 1976.

Appendix D
SOME STATISTICAL FLUCTUATION MODELS BASED ON ACOUSTIC MECHANISMS

As discussed in Volume I, it is common practice in performance analyses to model signal or noise or signal-excess fluctuations as stochastic processes. The choice of a specific process may be based on experience but usually tends toward mathematical convenience. What follows is a review of some of the theoretical treatments of fluctuations based on acoustic mechanisms. The corresponding statistical properties are listed so that they can be noted in the test cases of Volume I. At the same time, stochastic-process models alternative to the usual ones (Appendix E) are proposed.

The scope of this effort does not allow for a complete survey of acoustic fluctuation models. Hence, the focus is on models for low-frequency signals which have multipath propagation as primary fluctuation mechanism and on noise models driven by the same multipath interference from multiple sources.

D.1 Quantities Modeled

Consider first exactly what parameters are to be modeled. For the types of sonar systems considered in this study the important quantities are the signal (S), noise (N), and S+N intensities resulting from array beamforming and narrowband filtering followed by squared-envelope averaging (see Appendix F). In addition, proper modeling

of the detector requires prediction of the properties of $\hat{N}$, an estimate of N derived from samples in neighboring filter bands or azimuth beams or time windows. There is, however, rationale for simulating performance with a detector that thresholds on S/N. For stable source levels and beam response, the quantities of interest are S, N, $\hat{N}$, S+N, $S/\hat{N}$, $N/\hat{N}$. Signal intensity (S) is then identified with transmission ratio (TR), the ratio of received intensity to source intensity ($10 \cdot \log TR = TL$).

Note that these quantities are usually formulated in dB's. The random-process models are most often applied to $10 \cdot \log S$ or $10 \cdot \log N$ or $10 \cdot \log (S/N)$ (relative to some reference intensity), so that a Gaussian distribution of the fluctuations of one of these variables means a log-normal distribution of the intensities. A great deal of care must be taken in converting statistical properties from intensity to dB units, and some further discussion is given below.

D.1.1 Intensity and Decibel Units

Let X be an intensity variable and L be the corresponding dB variable:

$$L = 10 \cdot \log(X/X_o) \equiv A \ell n X,$$

where X_o is reference intensity (unity here) and $A = 4.34$. If X has distribution function $F(c) = P(X \leq c)$, then L's distribution function is G,

$$G(d) = P(L \leq d) = P(X \leq e^{d/A}) = F(e^{d/A}), \qquad (D\text{-}1)$$

and

$$F(c) = P(X \leq c) = P(L \leq A\ell nc) = G(A\ell nc). \qquad \text{(D-2)}$$

The density functions are related by

$$g(d) = f(e^{d/A}) \cdot \frac{1}{A} e^{d/A}, \qquad \text{(D-3)}$$

and

$$f(c) = g(A\ell nc) \cdot \frac{A}{c}. \qquad \text{(D-4)}$$

Hence X and L have significantly different density functions.

To display distribution properties of X or L it is often sensible to use order statistics, which are invariant under monotone (increasing) transformations. For example, the 20th percentile for X is c(.2), defined as

$$P[X \leq c(.2)] = 0.2.$$

The same percentile for L is d(.2),

$$P[L \leq d(.2)] = 0.2,$$

so that

$$d(.2) = A\ell n[c(.2)].$$

Hence, given percentiles of X, those of L are easy to find. On the other hand, moments are not easy to convert. In general

$$E(X^k) = \int x^k f(x)dx$$

and

$$E(L^k) = \int y^k g(y)dy = \int y^k f(e^{y/A}) \cdot \frac{1}{A} e^{y/A} dy,$$

so that $E(L^k) \neq A\ell n[E(X^k)]$. There is seldom an easy way to determine even the mean value of the transformed variable.

Consider next the scale and location parameters of X and L. Suppose that X's density function depends on a location parameter a and a scale parameter b:

$$F(x) = \hat{F}(\frac{x-a}{b}).$$

Then

$$G(y) = F[\exp(\frac{y}{A})] = F\left(\frac{\exp(\frac{y}{A})-a}{b}\right)$$

$$= \hat{F}[\exp(\frac{Y-A\ell nb}{A}) - \frac{a}{b}],$$

so that $A\ell nb$ becomes a location parameter for L, while $(\frac{a}{b})$ remains a shape parameter. The importance of this observation is that in using L as a fluctuation variable, it is usual to set its mean (or median) to 0, and/or assume that X_o is an arbitrary reference for X. In either case, the scale parameter of X and the location parameter of L are treated as arbitrary. A good example is in the exponential distribution for X (see Ref. D-1):

$$F(x) = 1-\exp(-x/\mu). \qquad \text{(D-5)}$$

Then

$$G(y) = 1-\exp[-(\exp(y/A))/\mu]$$

$$= 1-\exp[-(\exp(\tfrac{1}{A})(y-A\ell n\mu)], \qquad \text{(D-6)}$$

which means that while X has mean μ and variance μ^2, L has variance and shape <u>independent</u> of μ:

$$E(L) = 10\log\mu + 2.5$$

$$Var(L) = (5.6)^2$$

D.2 Signal Fluctuations

Consider next some intensity distributions which result from the conditions of a moving source in a multipath environment. The usual ray formulation for signal multipaths is

$$s(t) = \sum_n A_n \exp[i(\omega t - k_n r + \phi_n)] \qquad \text{(D-7)}$$

where $k_n = k\cos\theta_n$, k is wavenumber, r is range, ω is angular frequency, θ_n is ray angle at the source, and ϕ_n is a "random" phase angle. Intensity is then proportional to

$$\frac{1}{T}\int_0^T s(t)s^*(t)dt, \qquad \text{(D-8)}$$

and the distribution is found by sampling in range, r.

D.2.1 Gamma and Chi-Square Distribution of Intensity

A number of important references (Physics of Sound in the Sea [1946], Dyer [1970], Mark [1972], Whalen [1971]) formulate models of signal (or transmission ratio) fluctuations which result in a Gamma distribution for the intensity.

Reference (D-2) uses the classical random-phasor approach. The signal pressure after filtering is assumed to have form

$$s = A\exp(i\theta) = \sum_j A_j \exp(i\theta)$$

where θ_j and A_j are real and random. Now, for

$$X = \mathrm{Re}(Ae^{i\theta}) = \sum_j \mathrm{Re}(A_j \exp(i\theta_j))$$

$$Y = \mathrm{Im}(Ae^{i\theta}) = \sum_j \mathrm{Im}(A_j \exp(i\theta_j)),$$

a central-limit theorem is assumed to apply, so that X and Y are normal and independent with mean zero and variance σ^2. The signal envelope $q = \sqrt{X^2+Y^2}$ then has Rayleigh density:

$$f_q(x) = \frac{x}{\sigma^2}\exp(-x^2/2\sigma), \text{ for } x \geq 0.$$

The signal intensity has the distribution of q^2, namely

$$f_{q^2}(x) = \frac{1}{2\sigma^2}\exp(-x/2\sigma^2) \qquad \text{(D-9)}$$

This is the exponential distribution or gamma distribution with 2 degrees of freedom (2 d.f.). When $\sigma = 1$, q^2 is a chi-square variable with 2 d.f.

Dyer [1970] has a more precise derivation. Let the pure-tone signal pressure at the receiver have form

$$s(t) = s_o \tau \sum_{n=1}^{N} A_n \cos(\omega t - \phi_n),$$

and assume

$$s(t) = A(t)\cos[\omega t - \phi(t)]$$

where A and ϕ vary slowly over intervals of length T ($T >> \frac{2\pi}{\omega}$). The intensity is then proportional to

$$X = \frac{1}{T}\int_0^T s^2(t)dt = \frac{\tau_o^2}{N^2}\left[\left(\sum_n A_n \cos\phi_n\right)^2 + \left(\sum_n A_n \sin\phi_n\right)^2\right]. \quad \text{(D-10)}$$

For N large, the sums of (D-10) are nearly normal by a central-limit theorem for each of the three cases:

(i) $A_n \equiv A$ and ϕ_n uniform on $[0,2\pi]$,
$\{\phi_n\}$ is an independent set.
(No scattering, random travel time)

(ii) A_n random with $E(A_n) = A$ and $Var(A_n) << 1$,
ϕ_n uniform on $[0,2\pi]$,
$\{A_n\}$, $\{\phi_n\}$ independent.
(Random travel time and scattering)

(iii) A_n random with $E(A_n) = A$, $Var(A_n) \ll 1$,
ϕ_n random with $E(\phi_n) = 0$, $Var(\phi_n) \ll 1$,
$\{A_n\}$, $\{\phi_n\}$ independent.
(Scattering, but no travel-time randomness)

In (i) and (ii), the cosine and sine sums are independent and normal with the same distribution, so that X is exponentially distributed. Note here that the assumptions are that there are many multipaths (N large) and each has about the same intensity. Case (iii) gives a sum of squares of two different normal variables.

Mark [1972] extends the pure tone case to finite bandwidth and shows, under special assumptions, that the intensity has a gamma distribution with n d.f. where

$$n = \frac{2\mu^2}{\sigma^2} \simeq 2(\text{Time})(\text{Bandwidth}).$$

Nearly any book on signal processing (e.g., Whalen [1971] or Davenport and Root [1958]) models the filtered signal or noise pressure (voltage) as a zero-mean, Gaussian, narrowband, stationary random process of form

$$s(t) = x(t)\cos\omega t - y(t)\sin\omega t$$

Then x(t) and y(t) are also stationary, uncorrelated, Gaussian processes with mean zero. The envelope squared is

$$q^2 = x^2(t) + y^2(t) \qquad \text{(D-11)}$$

and has the exponential distribution.

This subsection concludes with some notes on the gamma and chi-square distributions (see, e.g., Cramer [1946]). If X_i are independent, normal variables with mean zero and variance $\sigma^2 = \frac{1}{2\beta}$, then

$$X = \sum_{i=1}^{n} X_i^2$$

is a gamma variable with n d.f. The density function is

$$p(x) = \begin{cases} \frac{\beta}{\Gamma(n/2)}(\beta x)^{n/2-1} e^{-\beta x}, & x > 0 \\ 0, & x \leq 0 \end{cases} \qquad \text{(D-12)}$$

with $E(X) = n/2\beta$, $Var(X) = n/2\beta^2$. The chi-square distribution is a special case of the gamma with $\beta=\frac{1}{2}$ or $\sigma^2=1$, while the exponential distribution is a chi-square or gamma with 2 d.f. The square-root of an exponential variable has the Rayleigh distribution.

For n fixed, the gamma distribution is a one-parameter family. In fact, a scale change $X \rightarrow (2\beta)^2 X$ converts a gamma variable to a chi-square variable. Hence, as discussed in D.1.1, for the log transformation of X with arbitrary reference intensity, chi-square variables can cover the general case.

As a final important note, the sum of independent chi-square variables is again chi-square (with the sum of the d.f.). Hence, the incoherent average of independent, identically distributed intensities can be modeled, to within a scale factor, as a chi-square variable.

D.2.2 Non-Central Chi-Square Distribution of Intensity

As seen above, the chi-square intensity results from multipath summation when the paths have nearly equal energy. A variation on this occurs when one path dominates (the "specular" path) and the other (the "scattered" field) shares the remaining energy about equally (Smith [1973] or Urick [1975]). The standard derivation dates to Rice [1945] or Nakagami [1943], but can be found in most signal-processing books (e.g., Ref. D-4 or D-5).

Let the "steady" signal

$$s_1(t) = A \cos(\omega t + \phi)$$

be added to a narrowband Gaussian noise (as in (D-10) above),

$$s_2(t) = x(t)\cos\omega t + y(t)\sin\omega t.$$

Then

$$s(t) = s_1(t) + s_2(t) \qquad \text{(D-13)}$$

$$= (x(t) + A\cos\phi)\cos\omega t - (y(t) + A\sin\phi)\sin\omega t$$

has envelope-squared (intensity)

$$q^2 = (x + A\cos\phi)^2 + (y + A\sin\phi)^2. \qquad \text{(D-14)}$$

The density function for q^2 is independent of the distribution of ϕ and is that of a non-central chi-square variable with 2 d.f.:

$$f_{q^2}(X) = \frac{1}{2\sigma^2}\exp\left(\frac{-(X+A^2)}{2\sigma^2}\right) I_o\left(\frac{2AX^{\frac{1}{2}}}{\sigma^2}\right). \qquad \text{(D-15)}$$

The envelope itself (normalized by σ) has the Rician density function:

$$f_{q/\sigma}(Y) = Y\exp[-(\frac{Y^2+A^2}{2})]I_o(Ay) \qquad \text{(D-15)}$$

Urick [1975] derives the same non-central chi-square distribution for intensity (Rician for RMS pressure) using a Rayleigh-phasor argument. McCabe [1976] has constructed a "log-Rice" random process simulation with GM processes and formula (D-14).

The sum of non-central chi-square variables (with noncentrality parameters the same) is again non-central chi-square, so that the incoherent average of intensities can be treated as a non-central chi-square variate (with appropriate d.f.). Notice also that as $A \to 0$, this variable becomes chi-square or gamma distributed. For about 5 or more d.f., the non-central chi-square is approximately normal for probabilities between 0.01 and 0.99.

Robertson [1969] has developed routines for calculating the non-central chi-square distribution. Whalen [1971] and others have calculated ROC curves based on this variable.

D.2.3 Temporal Properties

When source motion through the multipath field is the major cause of fluctuations, the temporal properties of signal are determined by the changes in transmission

loss with range and the range rate r(t) of the source.* In terms of (D-7) and (D-8), intensity is proportional to

$$I = \sum_n A_n^2 + \sum_{m \neq n} \sum A_m A_n \cos [(k_m - k_n) r(t) + \hat{\phi}_{mn}]$$

where

$$k_m - k_n = k(\cos\theta_m - \cos\theta_n).$$

When the RMS pressures, A_j, are of similar magnitudes, then the intensity fluctuations in range, r, are driven by terms of form

$$A_m A_n \cos[(k_m - k_n) r(t)].$$

Following Clay [1968], define a "spatial spectrum" for I as

$$I(k_m - k_n) = A_m A_n,$$

which identifies the dominant oscillations of I in range. A typical deep-water, long-range case at 25 Hz might yield a spectrum of the form shown in Figure D-1. The abscissa of the figure is given in units of cycles per range interval. To convert to a temporal scale, the range rate is incorporated: examples are given for a 3-knot and a 9-knot source in the figure.

---

*For $|r| \ll$ sound speed.

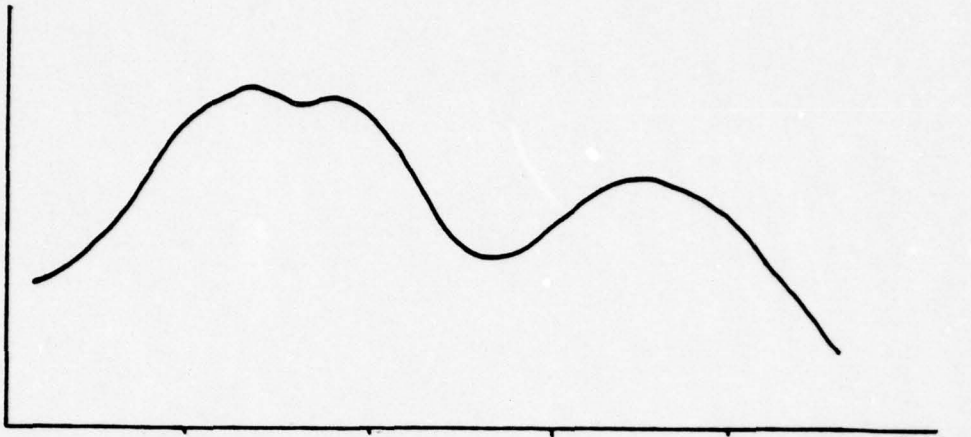

Range Spectrum

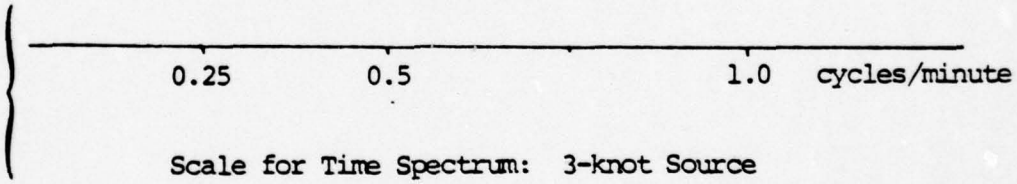

Scale for Time Spectrum: 3-knot Source

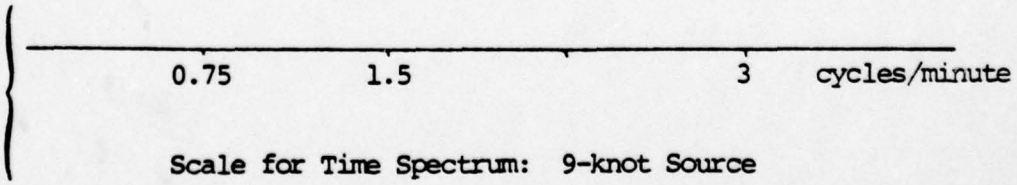

Scale for Time Spectrum: 9-knot Source

Transmission Fluctuation Spectrum

Figure D-1

Although some investigators have studied the fluctuation spectrum (e.g., Urick [1974]), many have concentrated on space/time "decorrelation" scales for signals (see, e.g. Smith [1976]) and the exponential autocorrelation function so prevalent in random-process modeling.

One alternative approach is discussed at length by Bendat [1958], the exponential-cosine autocovariance function:

$$C(\tau) = e^{-\lambda(\tau)}\cos\omega\tau. \qquad \text{(D-17)}$$

The reference gives a number of examples in physics for which (D-17) is appropriate. More important perhaps is the fact that combinations of two or more such functions give rise to spectra with two or more maxima - as is often seen in signal fluctuation data (e.g., Figure D-1).

Finally, it must be kept in mind that the temporal properties for intensity will in general be different from those of dB variables. In particular, there is no simple correspondence between autocovariance functions for the two quantities. But periodicities in one are periodicities in the other so that at least the dominant components of one spectrum should appear in the other.

D.3 Shipping-Noise Fluctuations

The multipath fluctuation models for signals can be extended and combined to yield models for the noise generated by distant ships. Some of these are summarized below.

D.3.1 Chi-Square and Non-Central Chi-Square Intensities

As mentioned in D.2.2, the standard signal-processor's approach to modeling narrowband noise (or signal) is to assume a stationary, Gaussian narrowband pressure, whose envelope-squared (intensity) is then a gamma variable with 2 d.f. The incoherent average of n independent samples leads to a gamma distribution with 2n d.f. In dB units this is equivalent to a chi-square variable with 2n d.f.

A justification for chi-square noise based on some physics is given by Dyer [1973] in an extension of his transmission fluctuation model. One approach to noise is to assume that a number of ships, say n, contribute about equally to the total noise intensity, that the sum is incoherent, and that each ship's signal consists of many multipaths of about equal energy. Then the noise intensity is the sum of n gamma variables with 2 d.f. and the same variance. In dB units this is equivalent to a chi-square variable with 2n d.f. Incoherent time averaging raises the number of degrees of freedom.

Similar reasoning for ship signals which have a non-central chi-square intensity (2 d.f.) results in a corresponding non-central chi-square distribution of intensity. The critical assumption in either case is that ships contribute equal energy to the total noise field. Such a situation is possible, but unlikely.

D.3.2 Distributions of Noise Intensities Related to Chi-Square

O'Connor [1973] and Dyer [1973] extend the model of D.3.1 to more general cases:

(i) the noise is the sum of N exponentially-distributed ship signals, each with different mean intensity.

(ii) the noise is the sum of N groups of ship signals, each group consisting of L_n equal-mean gamma variables.

The second case is the more interesting and general. The total noise intensity is then the sum of N variables

$$I = \sum_{i=1}^{N} Y_i$$

where Y_i is a gamma variable with mean μ_i and $2L_i$ d.f. The characteristic function of I is easy to find, but a non-numerical Fourier inversion is not available. O'Connor considers Edgeworth expansions and concludes that estimation of the distribution of I should involve

(a) numerical convolution of those Y_i with small L_i (say $L_i < 5$ or 10)

(b) approximation of Y_i by a Gaussian variable if L_i is large (say $L_i > 5$ or 10).

His results for several examples show intensity distributions which look like anything from a chi-square (2 d.f.) to a Gaussian (chi-square with many d.f.).

D.3.3 Temporal Properties

If ship contributions are independent variables, then the spectra and correlation functions add. A model such as suggested in D.2.3 would yield a weighted sum of exponential (or exponential-cosine) autocovariance functions to represent the noise autocovariance functions.

Another approach, developed specifically for beam noise by Goldman [1974] assumes that ships cross beams according to a shot-process, which in turn induces temporal correlation properties for beam noise. Resulting autocovariance functions depending on ship arrival densities and the beam pattern, but not on the details of TL, range from exponential to linear.

REFERENCES

D-1 Dyer, I., "Statistics of Sound Propagation in the Ocean," JASA 48, 337-345 (1970)

D-2 National Defense Research Committee Division 6 Summary Technical Reports, "Physics of Sound in the Sea" (1946)

D-3 Mark, W. D., "Statistics of Multipath Transmission of Finite Bandwidth Signals," J. Acous. Soc. Am. 52, 413-425 (1972)

D-4 Whalen, A. D., Detection of Signals in Noise, Academic Press, New York (1971)

D-5 Davenport, W. B. and Root, W. L., Random Signals and Noise, McGraw-Hill, New York (1958)

D-6 Cramer, H., Mathematical Methods of Statistics, Princeton U. Press, Princeton, N.J. (1946)

D-7 Smith, P. W., "Statistics of Fluctuations in Measures of Sound Propagated in Shallow Water," Bolt Beranek and Newman Report 2498 (1973)

D-8 Urick, R. J., "A Statistical Model for the Fluctuation of Sound Transmission in the Sea," Proceedings of the First Workshop on Operations Research Models of Fluctuations Affecting Passive Sonar Detection, DTNSRDC, Carderock, Md. (1975)

D-9 Rice, S. O., "The Mathematical Analysis of Random Noise," Bell Sys. Tech. J. 23, 282-332 (1944) and 24, 46-156 (1945). Reprinted in Noise and Stochastic Processes, N. Wax, ed., Dover, New York (1954).

D-10 Nakagami, M. "Statistical Characteristics of Short-Wave Fading," J. Inst. Elec. Commun. Engrs. Japan 239 (1943). [See, Statistical Methods in Radio Wave Propagation, Pergamon Press, New York (1960)]

D-11 McCabe, B. J., "A Stationary Stochastic Process with Log-Rice Distribution and Continuous Sample Paths," Interim Memorandum to ONR, D. H. Wagner Associates (1976)

D-12 Robertson, G. H., "Computation of the Noncentral Chi-Square Distribution," Bell Sys. Tech. J. 48, 201-207 (1969)

D-13 Clay, C. S., "Interference of Arrivals in Continous Wave Transmission Experiments," Meteorology International Inc., Tech Note Four Project M-153 (1968)

D-14 Urick, R. J., "Fluctuation Spectra of Signals Transmitted in the Sea and Their Meaning for Signal Detectability," NOLTR 74-156, Naval Ordnance Lab (1974)

D-15 Smith, P. W., "Spatial Coherence in Multipath or Multimodel Channels," J. Acous. Soc. Am. 60, 305-310 (1976)

D-16 Bendat, J. S., Principles and Applications of Random Noise Theory, Wiley, New York (1958)

D-17 Dyer, I., "Statistics of Distant Shipping Noise," J. Acous. Soc. Am. 53, 564-570 (1973)

D-18 O'Connor, J. C., "Statistics of Sea Noise," MIT Thesis (1973)

D-19 Goldman, J., "A Model of Broadband Ambient Noise Fluctuations Due to Shipping," Bell Laboratories OSTP-31JG (1974)

Appendix E

STOCHASTIC FLUCTUATION MODELS USED IN OPERATIONS ANALYSIS

This Appendix describes some of the random-process fluctuation models in common use for performance and engagement modeling, their properties, and the rationale for selecting certain ones for testing in this study.

E.1 General Types and Properties

Nearly every performance and engagement model in current use simulates detections on signal-to-noise ratio (SNR) or the closely-related signal excess (SE), and hence focuses on modeling fluctuations for one of these variables. There are two basically different approaches:

(a) Total SE. Here the SE fluctuations are assumed to have a composite statistical description representing the sum of the components. An example is the classical surveillance model in which the single-glimpse detection probability and false alarm probability are found from ROC curves parameterized on SE or SNR and based on assumptions about the fluctuation distributions and processor performance. With the single-glimpse model there is an associated time between independent glimpses. Then both instantaneous and cumulative detection probabilities can be calculated as functions of mean values of SE or SNR directly.

(b) Components. In this case, fluctuations of the components of the sonar equation are modeled individually, and then combined to yield the total description (SNR or SE).

These two approaches may be mathematically equivalent, but suggest different levels of modeling detail. In the first,

no attempt is made to determine the dominant contributors to the fluctuating SE, while the opposite is presumably true for the second.

Given a random process model for fluctuations in SE(t) of either type, the next consideration concerns the estimation of system performance. As mentioned in Appendix B, the primary MOE's are related to level crossings of SE(t), e.g.,

- $P[SE(t) > 0]$, the instantaneous detection probability at time t
- $P[SE(s) > 0$ for some $s \leq T]$, the cumulative detection probability
- $P[SE(s) > \alpha$ over some interval of length T_1 or $SE(s) > \beta$ over interval of length $T_2]$

Calculation of such quantities requires the joint probability distribution functions of SE(t) of all orders*:

$$P[SE(t_1) \leq A_1,\ SE(t_2) \leq A_2,\ \ldots,\ SE(t_k) \leq A_k] \qquad \text{(E-1)}$$

for every k and all sets of $\{t_i\}$ and $\{A_i\}$.

Even when these are explicitly known, level-crossing statistics can be difficult to evaluate, and numerical integration or Monte-Carlo simulations must be employed. The description of the random process models below will concentrate on properties which affect the calculation of (E-1) and level-crossings.

*Cases can be contrived where even this is insufficient.

E.2 Some Popular Stochastic-Process Models

The stochastic models to be described here have, for the most part, no basis in the physics of signals or noise, and thus have been used in an all-purpose mode - to simulate SE as well as the component signal and noise. Hence, in this appendix Z(t) will denote the quantity to be simulated and X(t) the random-process fluctuation model for Z. In particular, we follow the usual approach in specifying Z(t) as

$$Z(t) = \overline{Z(t)} + X(t) \qquad \text{(E-2)}$$

where $\overline{Z(t)}$ is the "deterministic part" of Z (some kind of averaged value) and X(t) is the "random part" or fluctuation term appropriate to the choice of $\overline{Z}$. These quantities are in dB units, but the sum is as indicated (i.e., not a power sum).

X(t) is usually modeled as a zero-mean process, implying that

$$E[Z(t)] = \overline{Z(t)} \qquad \text{(E-3)}$$

However, in a few cases $\overline{Z}$ is derived from a power average, i.e.,

$$Z(t) = 10 \log I(t)$$

$$\overline{Z(t)} = 10 \log [E(I(t))]$$

so that

$$X(t) = 10 \log [I(t)/E(I(t))]$$

may have a non-zero, t-dependent mean.

As a final note, the ultimate use of these models is to determine detection performance. In view of the MOE's mentioned above in E.1, the probabilities of interest are of the type:

$$P[Z(t_0) > \hat{M}]$$

$$P[Z(t) > \hat{M} \text{ for } 0 \leq t \leq T]$$

$$P[Z(t) > M \text{ for some interval length } T_0 \text{ in } 0 \leq T_0 \leq T]$$

$$P[Z(t) > \hat{M} \text{ for some } t \text{ in } (0,T)].$$

But these constant threshold-crossing probabilities for Z(t) become, from (E-2), variable threshold problems for X(t) whenever $\overline{Z(t)}$ is non-constant, i.e.,

$$P[X(t) > \hat{M} - \overline{Z(t)} \text{ for } t...] \equiv P[X(t) > M(t) \text{ for } t...]. \qquad \text{(E-4)}$$

E.2.1 Stationary, Continuous-Parameter Gauss-Markov Process (GM Process)

The definitions of Appendix A and the title fully describe the GM random process. Additional properties are discussed in References E-1 through E-5, and are summarized below:

- Sample functions are continuous, but nowhere differentiable.

- Since the process is Markov, all distribution functions can be determined from the second order density function for the zero-mean process:

$$f(x,y;t,t+\Delta)$$

$$= \frac{1}{2\pi\sigma^2(1-w)^{\frac{1}{2}}} \cdot \exp\left[\frac{-(x^2-2wxy+y^2)}{2\sigma^2(1-w)^2}\right] \qquad \text{(E-5)}$$

where

$$w = E[X(t)X(t+\Delta)]/\sigma^2 = e^{-\lambda|\Delta|}$$

and

$$\sigma^2 = E[X^2(t)].$$

Hence, the process is determined uniquely by three parameters:

$$\mu = E[X(t)],\ \sigma^2 > 0, \text{ and } \lambda \geq 0.$$

- The conditional density function for the zero-mean process is normal:

$$f(y;t+\Delta|x;t) = \frac{1}{\sqrt{2\pi}\sigma(\Delta)} \exp\left(\frac{-[y-\mu(\Delta)]^2}{2\sigma^2(\Delta)}\right) \qquad \text{(E-6)}$$

with $\mu(\Delta) = xe^{-\lambda\Delta}$ and $\sigma^2(\Delta) = (1-e^{-2\lambda\Delta})\cdot\sigma^2$.

- The marginal density of X(t) for fixed t is

$$f(x;t) = \frac{1}{2\pi\sigma} \exp\left(\frac{-(x-\mu)^2}{2\sigma^2}\right)$$

- The autocovariance function is

$$C(t_1, t_1+\Delta) \equiv \sigma^2 e^{-\lambda|\Delta|} \equiv C(\Delta),$$

while the autocorrelation function is

$$R(t_1, t_1+\Delta) = e^{-\lambda|\Delta|}\sigma^2 + \mu^2 \equiv R(\Delta).$$

- The process is stationary in the strict (and hence also wide) sense.

- If X(t) is a zero-mean process and $\lambda > 0$, then it is ergodic, since

$$\int_{-\infty}^{\infty} |R(t)|dt = \sigma^2 \int_{-\infty}^{\infty} e^{-\lambda|t|}dt = \frac{2\sigma^2}{\lambda} < \infty$$

[or, see Eq. (E-6)].

- For E(X)=0, the power spectrum of X(t) is

$$S(w) = \int_{-\infty}^{\infty} R(t)e^{iwt}dt = \frac{2\sigma^2\lambda}{w^2 + \lambda^2} \qquad \text{(E-7)}$$

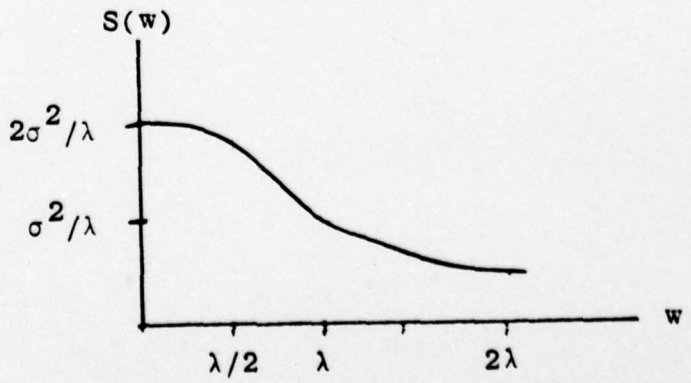

The power in the band $0 \leq w \leq L$ is then

$$\frac{\sigma^2}{\pi} \tan^{-1}\left(\frac{L}{\lambda}\right),$$

and hence the power over $-\lambda \leq w \leq \lambda$ is $\sigma^2/2$, while that over all frequencies is $\sigma^2 = E[X^2(t)]$.

It is usual to define $\tau = 1/\lambda$ as the <u>decorrelation time</u> or <u>relaxation time</u> of the process. Notice that half of the power corresponds to periods of $2\pi/\lambda = 2\pi\tau$ or greater and 90% of the power corresponds to periods of τ or greater. Of course, "power" here may have no relationship with physical power.

Note that the short-time average of a GM process is not a GM process. In fact, if $\varepsilon > 0$ and

$$Y(t) = \frac{1}{2\varepsilon} \int_{t-\varepsilon}^{t+\varepsilon} X(\tau)d\tau,$$

then Y is Gaussian (since a linear transform of X) but has spectrum

$$S_y(w) = \left(\frac{2\lambda^2}{\lambda^2 + w^2}\right)\left(\frac{\sin^2 \varepsilon w}{(\varepsilon w)^2}\right)$$

The limited analytic level-crossing results for GM are summarized in Ref. E-6. Various zero-crossing and density-of-maximum formulae can be found in Ref. E-3. A

method for generating simulated GM sample functions (at discrete points in time) is derived from Eq. (E-5) and described in Appendix H.

In addition to its mathematically convenient description, the GM process is attractive as a model of fluctuations for reasons related to physical processes. The Gaussian process has seen many applications, from particle physics (see Ref. E-2) to communications engineering. On the latter, Rice (Ref. E-5) defines white Gaussian noise in terms of simple oscillations and notes that a stationary Gaussian process can be viewed as the output of a linear system receiving such noise. A stationary GM process is the result of passing white noise through an RC filter (Ref. E-3).

E.2.2 Poisson Step or Jump Process

A step or Jump process is defined as

$$X(t) = Y_{N(t)} \text{ for } t \geq 0,$$

where Y_0, Y_1, ... are independent random variables with a common distribution and the index function N(t) is a Poisson process for $t \geq 0$, $\lambda > 0$:

$$P[N(t)=k] = e^{-\lambda t} \frac{(\lambda t)^k}{k!}, \quad k=0,1,\ldots,$$

with $E[N(t)] = \lambda t$ and $Var[N(t)] = \lambda t$. Then N(t) is the number of steps or jumps in the process X(t), and $\tau \equiv 1/\lambda$, called the relaxation or decorrelation time of X, is the mean time between steps.

Without any further constraints on Y_i, a number of properties of X(t) can be stated (see Refs. E-1, E-3, E-4, and E-7).

- The sample functions are step functions, discontinuous at the time of a step.

- X(t) is strict-sense stationary and Markov.

- X(t) has autocovariance function $C(t) = \sigma^2 e^{-\lambda|t|}$, with $E[X(t)] = E(Y_i) \equiv \mu$ and $E[X^2(t)] = E(Y_i^2) \equiv \sigma^2$. Its spectrum is then the same as that of the GM process for $\mu=0$.

- The conditional (transition) density is

$$f(y;t+\Delta|x;t) = e^{-\lambda\Delta}\delta(y-x) + (1-e^{-\lambda\Delta})f_Y(Y) \quad \text{(E-8)}$$

  where δ is the Dirac function and f_Y is the density function for Y_i.

- The joint density function is

$$f(x,y;t,t+\Delta)=e^{-\lambda\Delta}\delta(y-x)f_X(x) + (1-e^{-\lambda\Delta})f_Y(y)f_X(x). \quad \text{(E-9)}$$

- From Ref. E-3, Eq. (E-9) shows that X is ergodic in the distribution function.

The step process is probably used more widely in sonar analysis than any other. The usual distribution for Y_i is the normal with $\mu = 0$, so that X(t) is determined

from two parameters (λ and σ), and then X is called a (λ,σ) Jump process. Note however that X is not a normal process since its second order density (E-9) is not normal, although its marginal distribution is. Even though the GM and (λ,σ) processes have the same one-dimensional distribution and autocorrelation function, the two processes can give quite different results in level-crossing problems (see Ref. E-8).

Like the GM process, the Poisson step process has seen numerous applications in physics and elsewhere - the reason being that waiting times (for something to happen) are reasonably Poisson-distributed. In addition, the process is easy to simulate, and there are a number of analytical solutions to level-crossing problems, including time to first passage above a general time-dependent level and time spent above a constant level (see Ref. E-7).

E.2.3 Combination GM-Step Process

Belkin and McCabe (Ref. E-1) introduced a family of processes

$$X_p(t) = pX_j(t) + \sqrt{1-p^2}\, X_G(t), \quad 0 \leq p \leq 1$$

which linearly combines the GM process (X_G) and the Jump process (X_J). It is argued that this mixture has the advantage of simulating both smooth and discontinuous fluctuations, and yet requires no more calculations to generate sample functions than the two component processes. Unfortunately, few analytical results have been discovered. Moreover, X_p has the popular exponential autocorrelation function only when

X_J and X_G have the same λ and σ. The factors p and $\sqrt{1-p^2}$ were chosen so that if X_J and X_G are zero-mean and independent, than $E(X_p)=0$, $E(X_p^2)=\sigma^2$, and $E[X_p(t)X_p(t+\tau)]=\sigma^2 e^{-\lambda|\tau|}$.

E.2.4 Ehrenfest Random Walk

The Ehrenfest process is substantially different from the GM or Step, but is used in sonar performance analyses (Ref. E-9) because it has properties similar to theirs.

The fluctuation variable X(t) is generated at discrete time steps $0,\tau\Delta t,2\tau\Delta t,\ldots,$ from

$$X(k\tau\Delta t) = \left(\frac{Y(k\Delta t)-n/2}{\sqrt{n/4}}\right)\sigma \qquad \text{(E-10)}$$

where Y is an Ehrenfest random walk. X is usually interpolated or held constant between time steps. The rest of X's properties are derived from those of Y.

The Ehrenfest random walk Y is a Markov chain, i.e., a discrete parameter Markov process with range equal to the set of integers $\{0,1,2,\ldots,n\}$. At each time step Y either increases one step or decreases one step from its last value, m, according to probabilities (1 - m/n) and (m/n) respectively. If Y(0) is chosen at random from a binomial distribution

$$P[Y(0) = k] = \binom{n}{k}\left(\frac{1}{2}\right)^n, \quad k = 0,1,\ldots,n, \qquad \text{(E-11)}$$

then Y is a stationary ergodic process with $E(Y) = n/2$, $Var(Y) = n/4$, a binomial one-dimensional density (E-11), and normalized autocovariance function $(1-2/n)^s$, where s is the number of steps. Thus, the variable in parentheses in (E-10) is a stationary, Markov chain with mean 0, variance 1, and autocorrelation function $(1-2/n)^s$. When the time step is given by

$$\Delta\tau = -\ln\left(1 - \frac{2}{n}\right),$$

then the decorrelation time is 1.

It is also important to note that Y's limited range implies that X is truncated at $\pm \sqrt{n\sigma}$. Moreover, since X has a binomial distribution, it approaches a normal variable for large values of n. Thus X approximates a truncated GM or Jump process in the sense that it has the same autocorrelation function, a one-dimensional distribution approaching Gaussian, and is an ergodic Markov process. On the other hand, it is unlike the other processes in that it has the sometimes desirable properties of being truncated and taking only a small jump at a time.

The Ehrenfest model was originally developed in connection with diffusion and heat exchange problems (see Ref. E-10). It is now used in the APSURV model (Ref. E-9), both for short-term and for long-term fluctuations.

E.2.5 Independent-Glimpse Model

The "independent-glimpse" model is nothing more than a set of probabilities of detection $P_D(\overline{SE},t)$, defined at discrete time steps $t_1, t_2, \ldots$, for a fixed false-alarm

probability and mean signal excess ($\overline{SE}$). It is then assumed that the probabilities can be accumulated according to the rule:

Probability of at least one detection during time interval $[T_1, T_2]$

$$= 1 - \prod_i [1 - P_D(\overline{SE}(t_i), t_i)],$$

with product over all t_i in $[T_1, T_2]$.

The values of P_D are derived from hypothesized ROC curves and the time intervals $(t_{i+1} - t_i)$ from experience. $\overline{SE}(t_i)$ is the average signal excess over the detection "glimpse," predicted with models of mean TL, noise, etc. and the sonar equation.

There are a number of possible underlying stochastic processes which would yield the above results. The most obvious approach assumes that signal and noise are random processes which give rise to the ROC curves (usually the standard Gaussian or Rayleigh curves) and which are independent at times $t_1, t_2, \ldots$ (see Appendix F).

This type of model has been used extensively in surveillance-system performance analyses, but seems to be giving way to others as more is learned about the properties of acoustic signals and noise. It should be noted, however, that it does not presume a SNR detector and, in its use of ROC's, attempts to correctly arrive at single-glimpse detection probabilities.

E.3 Summary

Of the five random-process models listed above, only three are addressed directly in this study: GM, (λ,σ)-Jump, and Ehrenfest. There are, of course, many other possibilities: the sum of several Ehrenfest processes or Jump processes, log-Rice processes, Jump models with other than Gaussian one-dimensional distributions, etc. Some of these and others based on acoustics considerations are cited in Appendix D as candidates for better simulations of signal or noise. However, the scope of this study is limited and it was decided that tests would be performed on the most popular and commonly-used approaches. The analysis of the acoustically modeled data, in Volume I, indirectly gives evidence for or against the validity of other processes.

REFERENCES

E-1 McCabe, B. J. and Belkin, B., "A Comparison of Detection Models Used in ASW Operations Analysis," D. H. Wagner Associates Report to ONR (1973)

E-2 Doob, J. L., Stochastic Processes, Wiley, New York (1953)

E-3 Papoulis, A., Probability, Random Variables, and Stochastic Processes, McGraw-Hill, New York (1965)

E-4 Feller, W., An Introduction to Probability Theory and Its Applications, Vol. II, Wiley, New York (1966)

E-5 Rice, S. O., "The Mathematical Analysis of Random Noise," Bell Sys. Tech. J. 23, 282-332 (1944) and 24, 46-156 (1945). Reprinted in Noise and Stochastic Processes, N. Wax, ed., Dover, New York (1954)

E-6 Mollegen, A. T., "Review and Comparison of Step Model and Gaussian-Markov Model," op. cit. (Ref. D-8) DTNSRDC, Carderock, Md. (1975)

E-7 Parzen, E., Stochastic Processes, Holden-Day, San Francisco (1962)

E-8 McCabe, B. J., "Consequences of Using a Gauss Markov Process Versus a Jump Process for Acoustic Fluctuations," D. H. Wagner Associates Report to COMSUBDEVGRU Two (1972)

E-9 APSURV Model Documentation, ASWSPO

E-10 Feller, W., An Introduction to Probability Theory and Its Applications, Vol. I, Wiley, New York (1957)

Appendix F
SIGNAL PROCESSOR AND DETECTOR SIMULATION

This Appendix discusses sonar-system detection models in general and gives rationale for the automatic SNR detector used in this study.

F.1 Detection of Narrowband Signals

Modern, low-frequency sonar systems have signal processors and displays geared to the detection of narrowband signals. In particular, the design is usually based on the assumption of white, Gaussian noise and slow Rayleigh-fading signals.*

Signal - The signal pressure (or voltage) is represented as a stationary random process

$$s(t) = A \cos(\omega t + \phi)$$

where the amplitude (A) is Rayleigh distributed, the phase (ϕ) is uniformly distributed over $[0, 2\pi]$, ϕ and A are independent, and the angular frequency (ω) is constant. These conditions are assumed to hold over a time interval of length T_1, which depends on the details of the source, geometry, and transmission medium. Over a second time scale of length T_2 the signal is assumed to have the special property

*See, e.g., Ref. F-1 or F-2 or F-3 for more rigorous definitions and analysis.

that ϕ and A are nearly constant and are independent from interval to interval, with $T_2 < T_1$ and $T_2 > 2\pi/\omega$. This describes the slow Rayleigh-fading, narrowband signal.

Noise - The noise pressure is assumed to be white and Gaussian.

The optimal detector is then one which performs the following operations:

(i) The input voltage v(t) is processed by a quadrature receiver (or matched-filter plus envelope detector) over n time intervals of length T_2 to yield q_i, i = 1, 2, ..., n. Here $nT_2 \leq T_1$ and each q_i^2 has form

$$q^2 = \left(\int_{T_2} V(t) \cos \omega t \, dt \right)^2 + \left(\int_{T_2} V(t) \sin \omega t \, dt \right)^2 . \qquad \text{(F-1)}$$

(ii) An estimate of the noise at the quadrature receiver output is made and a threshold (TH) set for a given false alarm probability.

(iii) A detection is called if

$$\frac{1}{n} \sum_{i=1}^{n} q_i^2 \geq TH,$$

and dismissed otherwise.

Notice that for A and ϕ constant over the T_2 - time interval, the quadrature receiver operating on signal alone gives $q^2 \approx A^2/2$. Hence q^2 is proportional to the average power or intensity of the signal. On the other hand, q^2/T_2 is an approximation to the mean of the power spectral density:

$$\lim_{T\to\infty} \frac{1}{T} \left| \int_{-T/2}^{T/2} v(t)\,(\cos\omega t + i\sin\omega t)\,dt \right|^2$$

so that $(q^2/T_2)\cdot(\Delta\omega/2\pi)$ approximates the power in the band $(\omega,\ \omega + \Delta\omega)$ and is again proportional to the acoustic intensity in that band. In most of what follows, q^2 will be associated with the intensity of the signal-plus-noise or noise at the processor output.

As an alternative to the quadrature receiver, a filter matched to the narrowband signal over interval $[0,T_2]$ gives

$$\int_0^t v(\tau)\cdot \sin[\omega(T_2 - t + \tau)]\,d\tau,$$

which has envelope equal to q. In practice, either an analog bandpass filter or a digital transform is used to estimate q. Many other variations for more complicated signals are possible, including adaptive filters or line trackers.

The estimate of q for the received pressure is derived from coherent processing. The phase of the signal pressure is important over the time period T_2 required to perform the integration. These coherent integration times may range from fractions of a second to several minutes, with the choice of time derived from best experience about the stability of the received signal, the bandwidth of the signal, and the accuracy requirements for the measurement. [On this last point, note that a rule of thumb based on the assumption that the spectrum is flat and that the time series of voltage can be represented by a random process with one-dimensional Gaussian distributions is that the power spectrum estimate is distributed as the multiple of a chi-square variable with $k = 2 \cdot (\text{Integration Time}) \cdot (\text{Bandwidth}) \equiv 2TB$ degrees of freedom. Hence, the variance of the estimate is about $(2/k) \cdot (\text{expected power})$.]

For step (ii), the threshold is set to limit the frequency of false alarms, i.e., to bound at some level the probability of calling a detection when signal is not present. Hence, an estimate of the noise level in the band of interest must be made. This could be accomplished in a number of ways, such as averaging the levels in neighboring frequency bands or time periods or directions, in essence assuming that these averages are of noise only rather than of signal-plus-noise. The thresholding rule then amounts to calling

a detection when the measured input exceeds the noise estimate by a certain amount.

Finally, in step (iii), the samples of q are incoherently averaged in time and then thresholded. The number of samples to be averaged will depend upon the time T_1 and subinterval time T_2. According to the rule of thumb given above, for T_1 fixed, the performance of the detector improves as coherent integration time T_2 is increased, provided of course that the signal stability assumptions hold.

The sequence described above leads to an optimal detector for the conditions stated. In practice, enhancement of performance or a requirement for more than instantaneous detection (e.g., holding, tracking) may call for more complicated rules, such as:

- call detection if the intensity exceeds a threshold for a given time period,
- call detection if *m* out of *n* samples exceed the threshold,
- reduce the threshold if a detection has occurred recently.

These might model the performance of a human operator viewing displays of narrowband filter output. Note that there may even be additional levels at which candidates (already detected by one of the above methods) are screened. For example, a detection might incorporate the classification

process, and hence require that certain lines already detected be correlated with known submarine signature characteristics.

The point to be made here is that proper simulation of the detection process is often nontrivial, involving human operator response, complex signal processing, and complicated detection rules. Some of the decision rules require information which cannot be modeled with confidence today, e.g., the frequency-bin-to-bin correlation of sea noise. Nonetheless, the coherent/incoherent processing sequence (i) - (iii) described above is viewed as a basic component of the processor algorithm.

F.2 Detecting With Signal-to-Noise Ratios

As mentioned in Appendix E, most system performance and engagement simulations model the detector as one which thresholds on time series of signal-to-noise ratio (SNR). In the last subsection, the actual detector operation was described in terms of the measurable quantities: signal-plus-noise and noise pressure. Specifically, if S + N and N are the signal-plus-noise and noise only outputs of the quadrature receiver, then the simplest realistic detector

(a) Estimates noise $\hat{N}$,

(b) Sets a threshold, TH, based on $\hat{N}$ so that $N \geq TH$ is unlikely,

(c) Compares received signal X with the threshold:

$X \geq (TH) \rightarrow$ conclude that $X = S + N$ and DETECT

$X < TH \rightarrow$ conclude that $X = N$ and NO DETECT

A related detector compares $S + N$ with $\hat{N}$ in place of (b) and (c):

$(\tilde{b})$ Select TH so that $N \geq (TH) \cdot (\hat{N})$ is unlikely,

$(\tilde{c})$ $X \geq (TH) \cdot \hat{N} \rightarrow$ DETECT

$X < (TH) \cdot \hat{N} \rightarrow$ NO DETECT

Now, the only direct way to associate a SNR detector with one of these is to make the assumption that the signal-plus-noise intensity $(S + N)$ can be separated into two additive terms, S and N, and that $\hat{N}$ is a good estimate of N. In that case,

$$S + N \geq (TH)\hat{N}$$

is nearly equivalent to

$$S/\hat{N} \geq (TH - 1), \quad \text{with } N/\hat{N} \simeq 1.$$

The same goes for the reverse inequality. But now a false alarm is impossible, i.e., a false alarm occurs if $N \geq (TH)\hat{N}$, but we have assumed $N \simeq \hat{N}$. Conditions under which the SNR detector makes sense in this context are:

(i) If S/N is very large and N is good, then $S + N \simeq S$, and false alarms are relatively unimportant for reasonable thresholds. This is an uninteresting case.

(ii) If S/N is not large, then under no class of conditions will coherent processing yield an intensity estimate of (S + N) which is like the sum of the intensities. However, if the signal and noise bandwidths are not comparable, then it is possible that incoherent averaging of the filter outputs will resemble a sum of signal and noise intensities.* It is not clear however that false alarms can be properly accounted for even in this case.

Condition (ii) is assumed to hold for this study, i.e., incoherent averaging follows the coherent integration. To illustrate the validity, consider Figures F-1 and F-2 which show ROC curves corresponding to the quadrature receiver performance for a slow Rayleigh-fading signal in white noise - first with no incoherent integration and then with much incoherent integration. In the first case, at any

---

*Let $s(t) = A \cos\theta \cos\omega t + A \sin\theta \sin\omega t$ and $n(t) = B \cos\hat{\theta} \cos\omega t + B \sin\hat{\theta} \sin\omega t$ be the signal and noise pressures, where A, B, θ and $\hat{\theta}$ are nearly constant over the filter integration time. Then the quadrature receiver outputs q^2 are

$$q_s^2 \simeq A^2/2,\ q_n^2 \simeq B^2/2,\ \text{and}\ q_{s+n}^2 \simeq \frac{A^2+B^2}{2} + AB[\cos(\theta-\hat{\theta})].$$

If the fluctuation rates of (A,θ) and $(B,\hat{\theta})$ are not comparable, then the average of the cross terms over time can vanish.

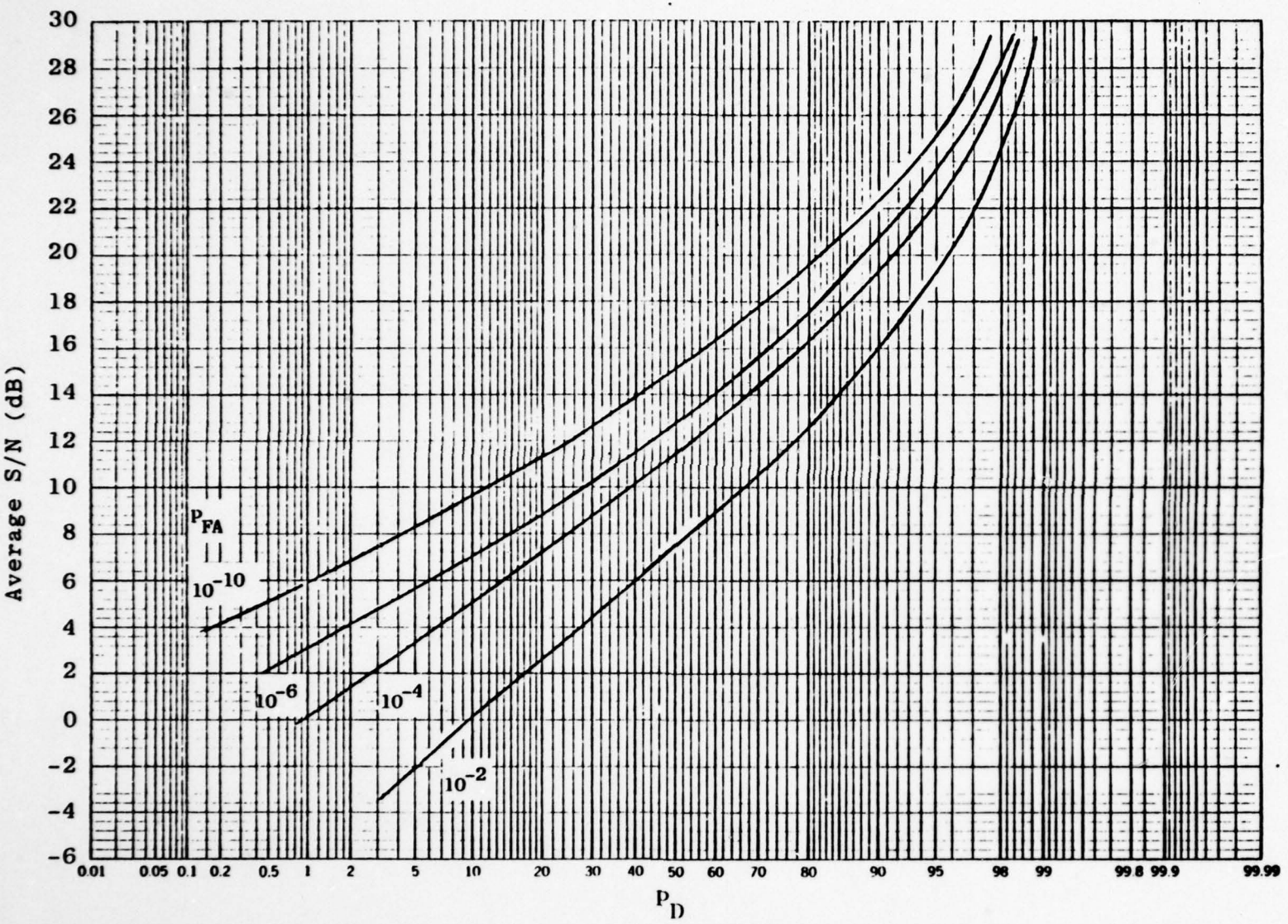

Figure F-1. ROC Curves - No Incoherent Averaging

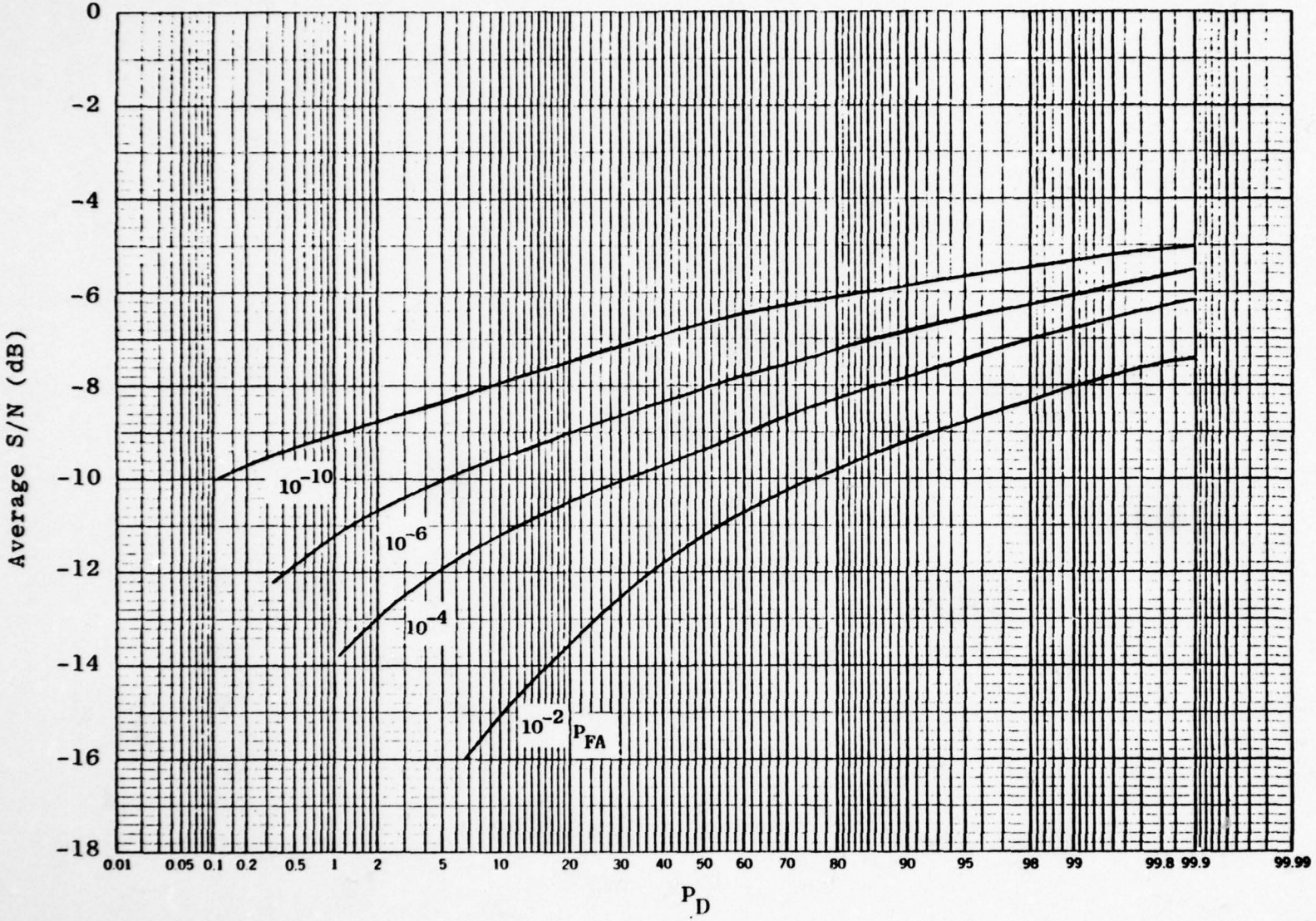

Figure F-2. ROC Curves - Much Incoherent Averaging

P_{FA}, S/N_o must change by many dB for P_D to rise from 0.1 to 0.9. In the second, at P_{FA} of 10^{-10}, P_D changes from 0.05 to 0.8 as S/N_o is increased from -8 to -6 dB. Hence, as a rough approximation, the SNR could be thresholded at -7 dB, with detection if SNR $\geq$ -7 and dismissal if SNR < -7. Thus, in essence, (S+N) has been separated into S and N.

F.3 Detector Models Used in This Study

Throughout this study an idealized detector is assumed. It correctly detects whenever the received signal-to-noise ratio (SNR) exceeds the fixed threshold for a prescribed time period and correctly dismisses otherwise. Here SNR represents the incoherently (time) averaged ratio of output signal power in the frequency band of interest to output noise power in that band.

With this detector as a basis, multi-level detectors of increasing complexity can be constructed:

- SNR must exceed one of several levels for an associated prescribed time period in order that a detection occur.

and/or

- Time-averaged SNR replaces SNR.

and/or

- Detection is delayed until the threshold is crossed m out of n times.

There are a number of reasons for selecting these detectors. First, they are "deterministic," so that all randomness is found in the inputs and the study can concentrate on the effects of various characterizations of acoustic fluctuations. Detection histories and associated statistics are easy to generate and reflect the details of the simulated SNR. Moreover, these algorithms mimic the performance of automatic detectors, as well as some aspects of human behavior. As mentioned above, multiple frequencies or classificatien questions are not considered - so these detectors may be viewed as the first stage of a higher level system. Finally, this set of detectors is a representative sample from the class of detectors currently used in performance/engagement analyses (see, e.g., Refs. F-3 through F-8). The single detector type which would round out the sample is one with variable threshold (either random or deterministic); but its study would complicate the extraction of detector sensitivity to the acoustic variables.

REFERENCES

F-1 Van Trees, H. L., Detection, Estimation, and Modulation Theory (Three Volumes), Wiley, New York (1968)

F-2 Whalen, A. D., Detection of Signals in Noise, Academic Press, New York (1961)

F-3 Gasteyer, C. E., "Passive Sonar Detection Processes in the SIM II Model," op. cit. (Ref. D-8) DTNSRDC (1975)

F-4 McCabe, B. J. and Belkin, B., "A Comparison of Detection Models Used in ASW Operations Analysis," D. H. Wagner Associates Report to ONR (1973)

F-5 Belkin, B., "Analytical Results for the Step Process and Gauss-Markov Process in Passive Detection Problems," op. cit. (Ref. D-8) DTNSRDC, Carderock, Md. (1975)

F-6 Mollegen, A. T., "Review and Comparison of Step Model and Gaussian-Markov Model," op. cit. (Ref. D-8) DTNSRDC, Carderock, Md. (1975)

F-7 APSURV Model Documentation, ASWSPO

F-8 APAIR Model Documentation, ASWSPO

AD-A055 676 SCIENCE APPLICATIONS INC MCLEAN VA F/G 17/1
ACOUSTIC FLUCTUATION MODELING AND SYSTEM PERFORMANCE ESTIMATION--ETC(U)
JAN 78 R C CAVANAGH N00014-76-C-0753
UNCLASSIFIED SAI-79-738-WA-VOL-2 NL

2 OF 2
ADA
055676

END
DATE
FILMED
8-78
DDC

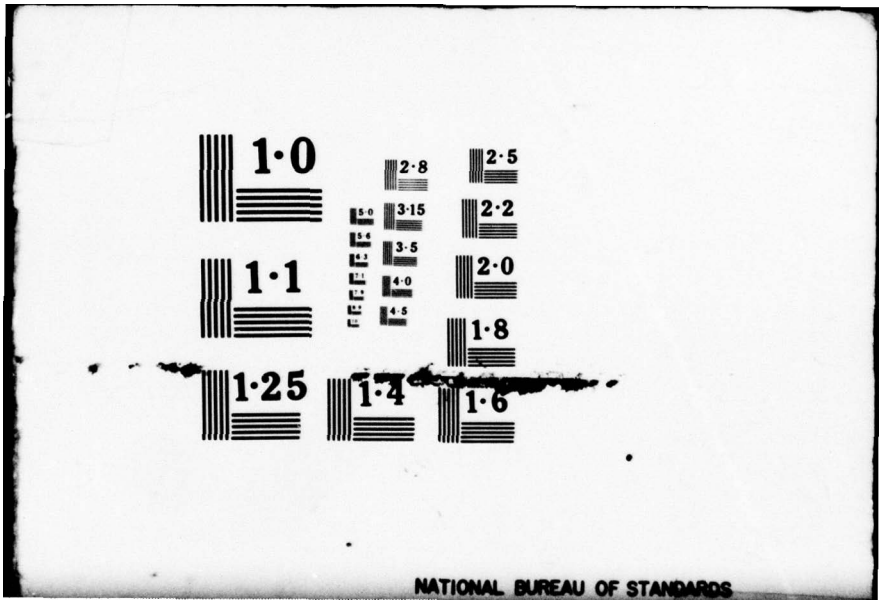
1·0
1·1
1·25
1·4
1·6
1·8
2·0
2·2
2·5
2·8
3·15
3·5
4·0
4·5
NATIONAL BUREAU OF STANDARDS

Appendix G

SOME ESTIMATES OF THE EFFECT OF THE ARRAY RESPONSE ON FLUCTUATIONS

This Appendix provides the justification for certain estimates used in Volume I of the effect of the array beam pattern on the fluctuations in signal and noise.

G.1 Effect of Array Response on Signal Fluctuations

Under the conditions of this study, the signal from a source moving across an array beam has fluctuations associated with

(i) the detailed transmission loss, TL(R), where R is radial range,

(ii) the array response, BP(ϕ) in dB's, where ϕ is azimuthal angle.

For the geometry shown below,

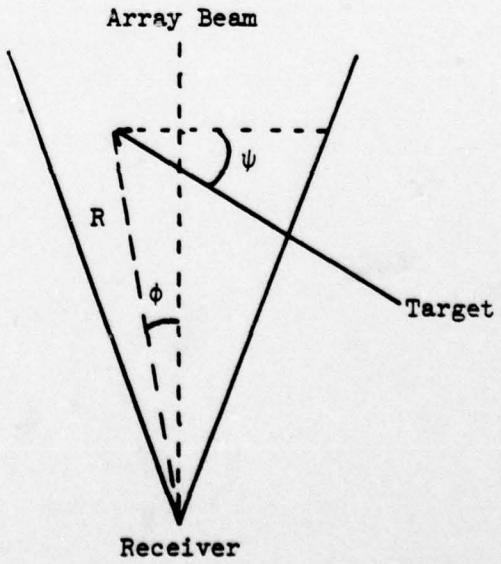

consider two extreme cases:

- The target moves across the beam at constant range ($\psi \approx 0$), and hence there are minimal TL fluctuations. The signal fluctuations are driven by BP(ϕ).

- The target moves in a radial direction from the receiver ($\psi \approx \pm 90^{o}$) and the signal fluctuations are those of TL(R).

At intermediate values of ψ, the two fluctuation mechanisms compete and it is desirable to know a priori which are important. The approach will be intuitive, relying on fluctuation periods and scales rather than on a rigorous treatment of the properties of TL(R) + BP(ϕ).

The array response function is of form $(\sin X/X)^2$ on the main beam, as described in Appendix H. Within the 6-dB-down beamwidth ($\Delta\phi$), the beam pattern function has range (spatial) period of about

$$\Delta\phi \cdot R$$

and a variance of about 4 dB. Then, as a target crosses the beam at angle ψ, the beam pattern function BP(ϕ) will vary with range along the target track and have period approximately equal to

$$\Delta\phi \cdot R/\cos\psi .$$

If the target speed is v, this converts to a temporal period of

$$\Delta\phi \cdot R/v \cdot \cos\psi$$

Typical examples for the test case of Volume I show TL with important spectral components at periods near 20-30 nm and 1-5 nm. Along the target track these convert to range periods (in nm) of

$$20/\sin\psi \text{ to } 30/\sin\psi \quad \text{and} \quad 5/\sin\psi \text{ to } 1/\sin\psi.$$

The "power" of each component depends on how the TL fluctuations are calculated, i.e., on the range-averaged $\overline{TL}$ which is removed and on the total range over which the TL is observed.

The interaction of the BP and TL fluctuation mechanisms can be observed in a number of ways. Consider here the normalized autocovariance function C(r) for

-TL + BP

and assume that TL and BP are uncorrelated. Then,

$$\sigma^2 C(r) = \sigma^2_{TL} C_{TL}(r) + \sigma^2_{BP} C_{BP}(r), \qquad \text{(G-1)}$$

where r is range lag and $\sigma^2 = \sigma^2_{TL} + \sigma^2_{BP}$. The corresponding Fourier transforms are:

$$\sigma^2 S(w) = \sigma^2_{TL} S_{TL}(w) + \sigma^2_{BP} S_{BP}(w).$$

Consider four cases:

Case 1: For ψ near 0, $\sigma^2_{TL} \approx 0$ and the signal fluctuations are driven by the BP variations.

Case 2: For $|\psi|$ near 90°, $\sigma^2_{BP} \approx 0$ and the signal fluctuations are driven by the TL variations.

Case 3: When the 5 nm-average $\overline{TL}$ is appropriate, i.e., fluctuation range periods are about $5/\sin\psi$ nm, then the BP and TL fluctuation periods are nearly equal for

$$5/\sin\psi \approx \Delta\phi \cdot R/\cos\psi$$

or

$$\tan\psi \approx 5/\Delta\phi \cdot R.$$

Then $\sigma^2_{TL} \approx 9$ dB and the important components of S_{TL} are at periods near $5/\sin\psi$ to $1/\sin\psi$. The BP term has $\sigma^2_{BP} \approx 4$ dB and $S_{BP}(w)$ with dominant component at $\Delta\phi \cdot R/\cos\psi$. Hence, the TL fluctuations may contribute significantly to the composite spectrum.

Case 4: When the radial change in target range is much greater than 5 nm, the test case shows TL with $\sigma^2_{TL} \approx 25$ or 30 dB and the 20-30 nm period dominates the spectrum. The BP fluctuations cannot distort the composite spectrum significantly.

For target speed v, the range periods mentioned above become time periods. Hence, when $|\psi| << 90^\circ$, the beam

response component has a variance of about 4 dB, a low frequency spectral contribution with a period of about

$$T \approx \Delta\phi \cdot R/v\cos\psi,$$

and decorrelation time

$$\tau \approx \Delta\phi \cdot R/2v\cos\psi.$$

The TL fluctuations are typically characterized by

Conditions	Target observed over short radial range interval (5 nm), but $\psi > 0$.	Target observed over large radial range interval.
σ^2	9 dB	30 dB
Dominant Periods	Power spread over periods 1 nm/vsinψ to 5 nm/vsinψ	Most of power at 20 nm/vsinψ to 30 nm/vsinψ
Decorrelation Times	0.5 nm/vsinψ	5 nm/vsinψ

The importance of the TL fluctuations compared to the BP fluctuations can be estimated in terms of these spectral components and powers.

The interaction of the two fluctuation mechanisms can also be viewed in terms of decorrelation times. Assume that TL and BP are independent, quadratic functions of range; then their autocovariance functions are linear and (G-1) becomes

$$\frac{\sigma^2}{\tau} = \frac{\sigma_{TL}^2}{\tau_{TL}} + \frac{\sigma_{BP}^2}{\tau_{BP}}, \quad \sigma^2 = \sigma_{TL}^2 + \sigma_{BP}^2 \qquad \text{(G-2)}$$

where τ is the decorrelation time of the total process and τ_{TL}, τ_{BP} are those for the components. As noted above,

$$\tau_{BP} \simeq \Delta\phi \cdot R/2v\cos\psi$$

and

$$\tau_{TL} \simeq \tau_r/v\sin\psi,$$

where τ_r is TL decorrelation range (e.g., 0.5 to 5 nm). Equation (G-2) can then be used to estimate τ and the relative importance of TL and BP. Take as an example the first case in the table above, but suppose σ_{TL}^2 corresponds to a shorter radial range interval and has value near that of $\sigma_{BP}^2 = 4$. Then

$$1/\tau = \tfrac{1}{2}(1/\tau_{TL} + 1/\tau_{BP})$$

and τ_{TL} will affect τ significantly when $\tau_{TL} << \tau_{BP}$ or

$$\tan\psi >> 2\tau_r/\Delta\phi \cdot R = 1/\Delta\phi \cdot R.$$

Thus, if $\Delta\phi = 8^\circ$, TL fluctuations will dominate BP fluctuations for

$$\psi >> 4^\circ, \text{ at } R = 100 \text{ nm},$$

and

$$\psi >> 1^\circ, \text{ at } R = 400 \text{ nm}.$$

If, in this example, σ^2_{TL} were 8 instead of 4, TL fluctuations would dominate when

$$\tau_{TL} << 2\tau_{BP},$$

or

$$\Psi >> 1/2\Delta\phi \cdot R.$$

These are very small angles for ranges of interest, and illustrate the importance of the detailed TL.

Such estimates are useful for obtaining order of magnitude approximations and further tests of the data are given in Volume I.

G.2 Multipath Beam Splitting

The response of the generic horizontal line array treated in this study and described in Appendix H is subject to distortion by multipath beam splitting when the array is steered away from broadside. The question then is: for signals arriving between vertical angles $\theta=0$ and $\theta=\theta max$ and for a fixed azimuthal beamwidth $\Delta\phi$, how far off broadside can an array be steered (ϕ_0) and yet have the signal appear on only one azimuthal beam?

On the main beam (Appendix H), the array intensity response is

$$I(\phi,\theta;\phi_0,\alpha) = \left(\frac{\sin y}{y}\right)^2$$

where

$$y = \alpha(\cos\theta\cos\phi - \cos\phi_0)$$

$$\alpha = (1.4)/\sin(\Delta\phi/2)$$

$\Delta\phi$ = main beamwidth (to half-power points) at broadside

ϕ_0 = steering angle, measured from endfire

ϕ = signal azimuthal arrival angle, measured from endfire

θ = signal vertical arrival angle, measured from the horizontal

If the array is steered to ϕ_0, then the arrival (θ,ϕ_0) will fall within the main beam (half-power points) if

$$\left(\frac{\sin y}{y}\right)^2 \geq 1/2,$$

or equivalently,

$$|\alpha(\cos\theta\cos\phi_0 - \cos\phi_0)| = |y| \leq 1.4.$$

A little arithmetic gives

$$|\cos\theta - 1| \leq [\sin(\Delta\phi/2)]/\cos\phi_0.$$

or

$$|2\sin^2(\theta/2)| \leq [\sin(\Delta\phi/2)]/\cos\phi_0. \qquad \text{(G-3)}$$

Values of $\theta_{max} > 0$ such that equality holds in (G-3) are plotted as a function of $\Delta\phi$ and ϕ_0 in Figure G-1.

For the cases studied here, $\Delta\phi = 4^\circ$ and 8°, all arrivals within 30° of the horizontal appear on the same beam as long as bearing angles are within about 35° of broadside.

G.3 Array Shading and Beam Noise

The choice for this study of a shaded horizontal line array with 30 dB sidelobe suppression is based on several considerations, one of which is the minimization of fluctuations in noise caused by sidelobe contributions (except, of course when the noise on the main lobes is extraordinarily low). The very simple rationale for selecting 30 dB is given below.

Suppose that the array noise output consists of two independent, normally distributed components (in dB's):

- the main-lobe contribution, N_1, with mean μ_1 and variance σ_1^2
- the total minor-lobe contribution, N_2, with μ_2, σ_2^2.

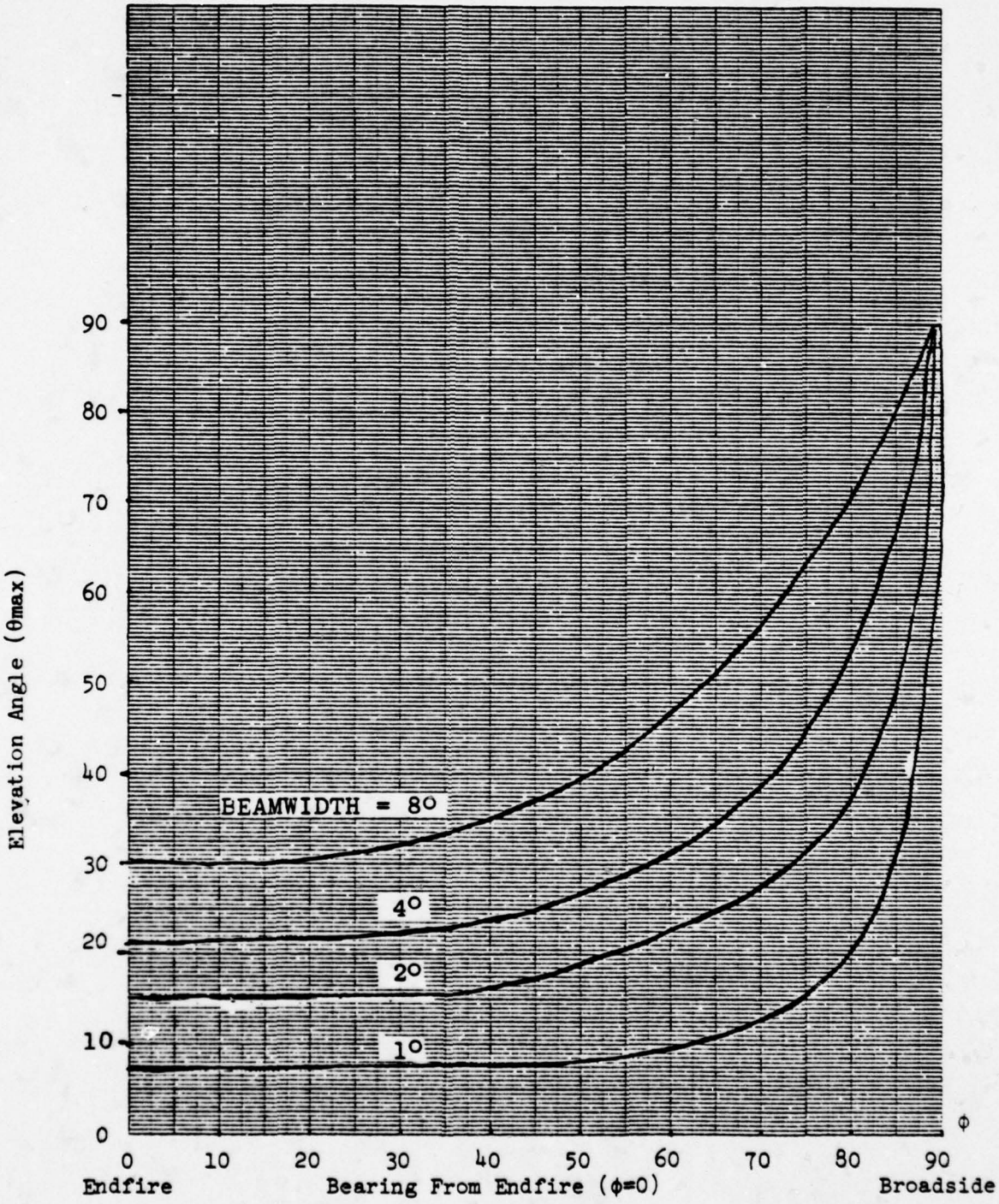

Maximum Vertical Arrival Angle Versus Bearing and Beamwidth

Figure G-1

To estimate the chances that the sidelobe noise contributes significantly to the total noise fluctuation, the probability that

$$N_2 > N_1 - TH,$$

must be estimated. Here TH is a "threshold" which determines the relative contribution of N_2. Since N_2 and N_1 add on an intensity basis (denoted " $\oplus$ "), $N_1 \oplus N_2 \leq (N_1 + 1)$ dB will hold if $N_2 < N_1 - 6$, or TH = 6 dB.

Experience with noise fluctuation distributions suggests 6 dB as an upper bound for σ_1 and σ_2. Furthermore, the mean levels are assumed to behave in the way expected of isotropic noise:

$$\mu_2 = \mu_1 + 10\log[(180-W)/W] - S,$$

where (W/180) is the fractional beamwidth for the main lobe and its ambiguous beam and S is the sidelobe suppression (in dB's). Letting BW = 10log (180-W)/W, N_2-N_1 is a normal variable with variance $\sigma^2 = 72$ and mean

$$\mu = \mu_2 - \mu_1 = BW - S.$$

Under these conditons, $P(N_2-N_1 > -TH)$ can be calculated, as shown in Table G-1.

The choice of S = 30 and use of 8^o beams in most of the study should then result in minimal noise fluctuation contributions from the sidelobes. Test results given in Volume I verify this.

TH	BW	W	S	$P(N_2-N_1 > -TH)$
6	13	8^o	35	0.02
6	16	4^o	38	0.02
6	13	8^o	32	0.05
6	16	4^o	35	0.05
6	13	8^o	29	0.10
6	16	4^o	32	0.10

Table G-1

Probabilities that Sidelobe Noise Exceeds Main Beam Noise

Appendix H
COMPUTER PACKAGES

A significant amount of computer software has been developed or exploited in pursuit of the objectives of this study. The various acoustic models, random-process models, and statistical analysis packages are described in this Appendix. No attempt is made to document the software in the usual sense; instead, the general capabilities, mechanics, and limitations of the packages, as well as their potential for further applications, are outlined here. All programs are coded in FORTRAN IV and are easily adapted to run on any large scale computer. The present version operates on CDC 6000 series machines.

H.1 Acoustic Models

The "acoustic" simulation of the beamformer-ouput time series consists of five distinct submodels: environment, receiving array, target, transmission loss, and surface ships. These components are combined according to the schematics of Figures H-1 and H-2 to simulate the time series of signal and noise as produced by the array beamformer. The signal and noise models, with each of their components, are examined below.

H.1.1 Signal, Noise Simulation Model (DSBN)

From Figures H-1 and H-2 it should be clear that the calculations for signal and noise time series are essentially the same, and are in fact both performed

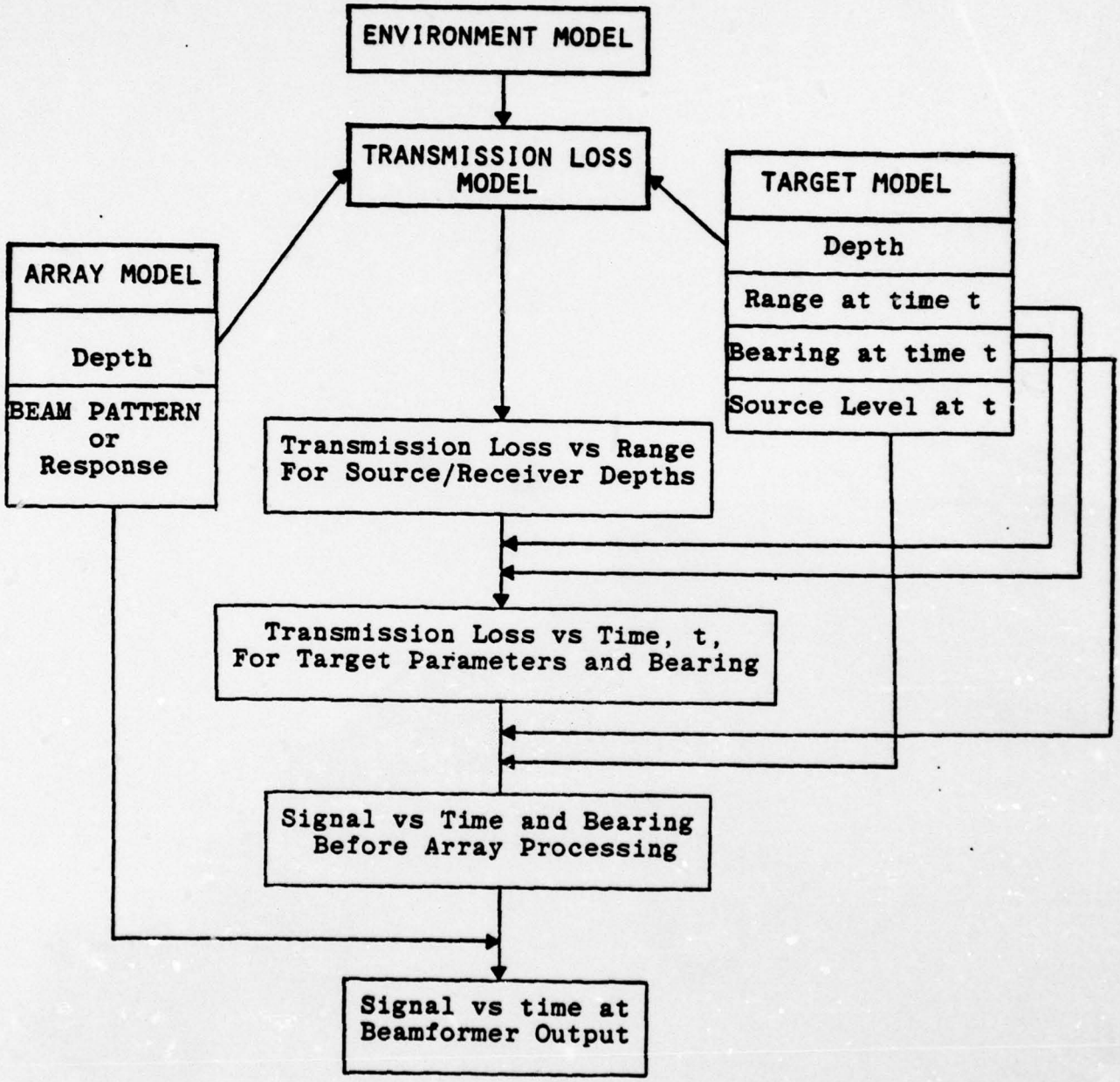

Figure H-1. Acoustic Signal Model

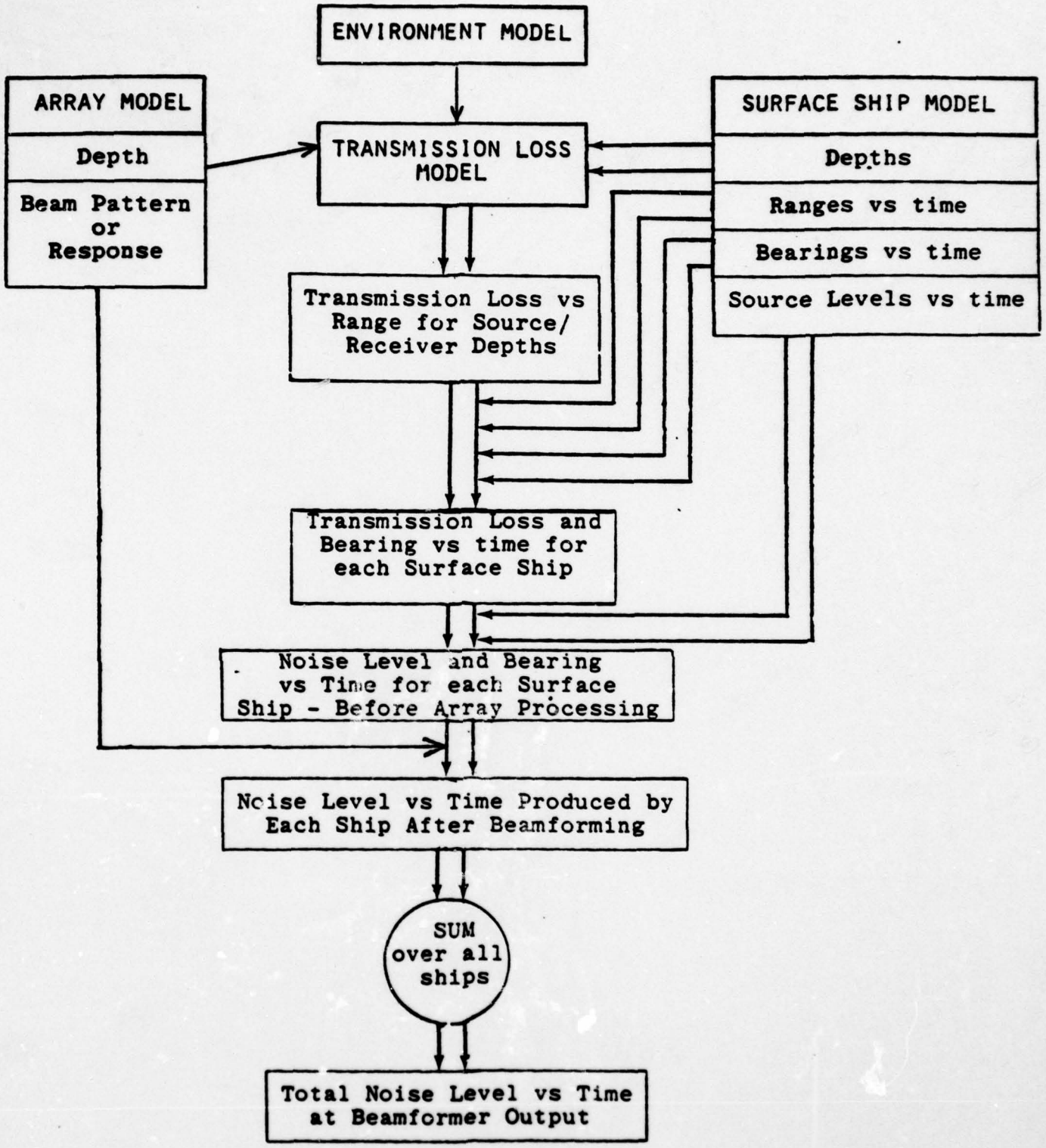

Figure H-2. Acoustic Noise Model

by the same routine called the "Discrete Shipping Beam-Noise" (DSBN) Model. The only difference between the signal and noise algorithms is that for signal there is a single target, while for noise there are many sources (targets) whose "signals" are summed incoherently. Two simple equations are the basis:

$$\begin{aligned}[\text{Signal Level at Time } t] &= [\text{Target Source Level at } t] \\ &+ [\text{Array Signal Gain for Target Bearing at } t] \\ &- [\text{Transmission Loss for Target Range and Bearing at } t] \end{aligned} \tag{H-1}$$

and

$$[\text{Noise Level at Time } t] = \sum \Big\{ [\text{Ship Source Level at } t] + [\text{Array Signal Gain for Ship Bearing at } t - [\text{Transmission Loss for Ship Range and Bearing at } t] \Big\} \tag{H-2}$$

Figure H-3 shows the computer-program flow. The noise or signal is computed at discrete time steps for each of ten (or fewer) array response functions. Readings are taken at prespecified time points (e.g., every minute) for a selectable time span (e.g., 30 hours). Now, the ship submodel provides the ship positions and source levels, the target submodel provides the target

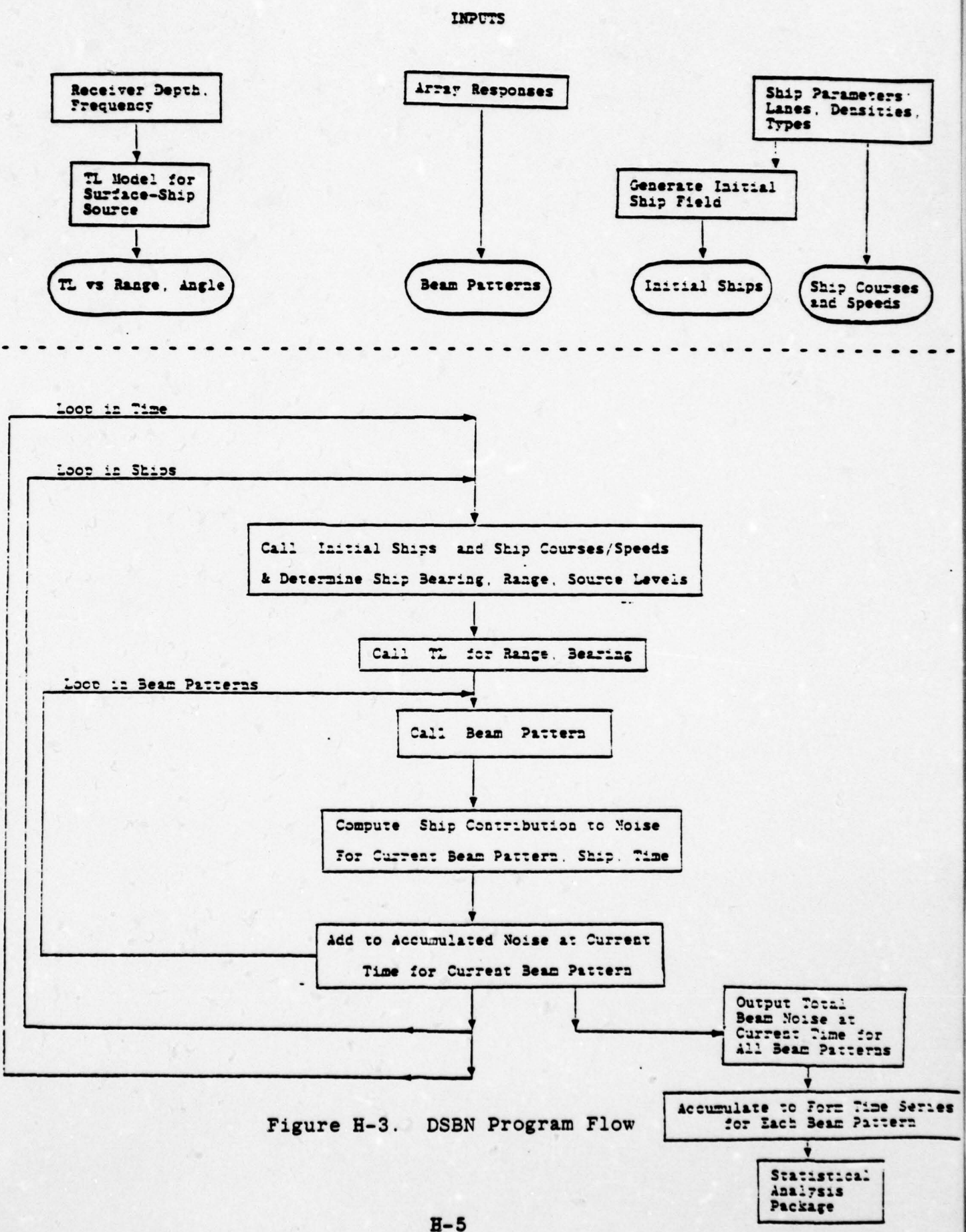

Figure H-3. DSBN Program Flow

positions and source levels, the environment and TL submodels provide the transmission loss from each source to the receiver, and the array submodel gives the response to a signal as a function of bearing. Hence, the outputs of these component submodels can be viewed as inputs to the main model, which in turn does no more than perform the simple geometry calculations and combine all the data according to equations (H-1) and (H-2).

The accuracy and quality of DSBN predictions are of course directly related to the quality of the inputs and component submodels. In addition, there are a few limitations associated with the DSBN Model Structure:

- The receiver array locations and source levels do not change with time.
- Only discrete point sources are allowed. Distributed sources could be simulated by many correlated point sources, but computer time would be prohibitive.
- There are dimension constraints, e.g., at most ten array response functions are allowed.
- Once the surface ship levels and courses are generated, all variables are deterministic.

- Only source positions change with time; other quantities (e.g., TL) depend on time only as induced by source motion.

Removal of these limitations requires a straightforward revision of the computer code.

H.1.2 Environmental Submodel

The environmental model (sound speed, bathymetry, bottom reflectivity, etc.) affects only the transmission loss portion of the acoustic simulation. Since the present version utilizes a time-independent TL, there is no provision for medium-induced fluctuations. The use of a time-varying environment may be of interest at some future date, but would require a significant expansion of the DSBN Model to accommodate a time-dependent TL.

H.1.3 Transmission Loss (TL) Submodel

DSBN requires from the transmission loss submodel the TL as a function of range from the receiver for all source/receiver locations and frequencies of the case under consideration. The present configuration of DSBN allows for the use of the vertical arrival structure (i.e., the loss as a function of range and vertical angle at the receiver) in order to model the three-dimensional response of an array. On the other hand, DSBN cannot utilize a TL function which depends on either bearing or time. The incorporation of such features amounts to a bookkeeping problem which could be solved directly if the detail were warranted.

Although a special TL submodel was used for this study (the Parabolic Equation model modified by inclusion of FACT-like bottom-bounce paths*), nearly any model which yields a table of transmission loss as a function of range will work. Of course, the TL function should exhibit detailed range-dependent structure if fluctuations are to be studied, and it should show proper source/receiver depth dependence.

For studies of source-motion-induced fluctuations caused by multipath interference, the range resolution in the TL model output depends on acoustic frequency, processor integration time, and the speed of the sources (i.e., the velocity component radial to the receiver). In the studies reported in Volume I, the TL sampling rate appropriate to 25 Hz, 2-minute integration times, and 15-20 knot speeds was found to be about 0.2 miles. The maximum range for ship contributions in the basin was assumed to be 500 miles. Thus, a typical TL table for low acoustic frequencies and open ocean has 500 x 5 = 2500 entries for <u>each</u> of the two or three source/receiver depth combinations. It should be clear that to incorporate time or bearing-dependent TL would require tables with perhaps 7500 x 10 to 7500 x 1000 entries. If arrival structure were included, multiply these figures by 10-100.

---

*See the discussion in Appendix C.

H.1.4 Array Submodel

For the present configuration of the DSBN Model, the array module is simply a functional giving the intensity response of the array to plane wave arrivals (i.e., a beam pattern). Since the test problem deals with a horizontal line array, the response is usually given in terms of azimuthal arrival angles. However, to investigate the effects of the horizontal array's vertical directivity away from broadside, the simulation model can accommodate a response function which depends on both azimuthal and vertical arrival angles.

For computation purposes, the user specifies the fixed location of the array and provides up to ten array-response functions corresponding to different steering angle orientations, shading, physical deformations, or whatever. The DSBN Model simulates beamformer output for each response function or beam pattern by modifying the intensity arrivals from ship sources or the target accordingly. The code also records the number of sources on the "main beam" defined below.

Two array functionals for DSBN have been programmed for this study and, because of their general applicability, are described next.

(a) Shaded Horizontal Line Array - Azimuthal Response Only

Intensity response at azimuthal angle ϕ is given by:

$$I(\phi;\phi_0,\alpha) = \begin{cases} \left(\frac{\sin x}{x}\right)^2 & \text{for } x \leq x_c \\ (10^{-D/10})\ (\sin x)^2 & \text{for } x > x_c \end{cases}$$

where $x = \alpha(\cos \phi - \cos \phi_0)$

$x_c = \pi(1 - 10^{-D/20})$,

ϕ_0 is "steering angle", measured from endfire

$\alpha = 1.4/\sin(\Delta/2)$

Δ = broadside beamwidth (to half power points)

D = "sidelobe suppression factor"

This function approximates the response of a shaded horizontal line array with main beamwidth Δ at broadside and with uniform sidelobe suppression (D dB down) with structure. x_c is constructed so that there is a smooth transition from the main lobe to the sidelobes.

(b) Shaded Horizontal Line Array - Vertical and Azimuthal Response

Here, the sidelobes are completely suppressed and the intensity response for azimuthal angle ϕ and vertical angle θ (re horizontal) is

$$I(\phi,\theta;\phi_0,\alpha) = \begin{cases} \left(\frac{\sin y}{y}\right)^2 & \text{for } y \leq \pi, \\ 0 & \text{for } y > \pi, \end{cases}$$

with $y = \alpha(\cos\theta \cos\phi - \cos\phi_0)$ and α, ϕ_0 as above.

Given that undistorted plane-wave response suffices, the primary limitation of the program is that the response function and array location cannot change with time. Such features can be added with minimal modifications to simulate, for example, the response of a transiting towed array which is changing orientation and suffering from physical deformation (wiggles).

A more basic limitation is that this array submodel does not apply directly to a predicted acoustic field which has not been decomposed into plane waves (e.g., output of the PE model in the vertical). The most efficient way to deal with this is to include the array response in the transmission loss by, in essence, inserting the array elements into the field and computing the beamformer algorithm directly.

H.1.5 Target Submodel

This module accepts as input a constant target source level, depth, course, and speed. It then tracks the target range and bearing to the receiving array as functions of time.

A straightforward modification to the program would allow for time-varying source level, course, and speed. Elimination of the constant-depth limitation would require significant changes in the way the TL model is used.

H.1.6 Surface Ship Submodel

The module which constructs surface ship positions and parameters can be viewed as having two parts. In the first part, the source levels, courses, and speeds are initialized as realizations of random variables. The second part simply tracks each ship's position and computes bearing and range to the array as functions of time, exactly as in the case of the target model. This tracking function is subject to the limitations listed in Section H.1.5.

Initialization of the ships and their parameters proceeds as follows. The user supplies constraints:

- Shipping "lanes" are specified by the distributions of speed and course and initial position, as well as an inter-arrival time interval (expected time between arrivals of ships across a line perpendicular to the mean lane courses).

- Source levels depend on the random speed, but also on another random variable (thought of as "length").

The present version of the DSBN model uses Poisson-distributed arrival times, so that the lane is expected to have an approximately uniform distribution of ships in range (i.e., constant density). The program uses a random number generator and the distribution functions to

produce a single replication of the shipping field with speeds, courses, locations, and source levels for each ship.

As in the target submodel, once the course, speed and level of a ship are selected, they remain constant for the duration of the replication time (e.g., 10 hours). For each subsequent replication, the initialization process is repeated.

There are, of course, other methods for generating ship distributions and tracks in the ocean. The one used here is very much like that of Ref. H-1 and not dissimilar from Ref. H-2.

H.2 Random-Process Models

One of the principal tasks of this study is the comparison of "acoustically-modeled" fluctuations with "stochastically modeled" fluctuations. Hence, time series of signal, noise, and SNR are generated first with the acoustic models described above, and then with some of the more popular random-process models. Selection of the random-process parameters mimics the procedures used in practice for engagement modeling (see Appendix E and Reference H-3). This subsection first discusses these procedures, and then describes some of the random-process simulation programs.

H.2.1 Procedures for Determining Random-Process Parameters

There are two different, but nearly equivalent, approaches: one for time series and the other for transmission loss.

H.2.1.1 Time series

The given time series is first subjected to a linear or other regression analysis to determine long-term trends. Note that this is usually performed in dB (log intensity) units, an important detail. If $X(t)$ denotes the time series and $\overline{X}(t)$ the trend (or "deterministic" part), then the "detrended" series is given by

$$Y(t) = X(t) - \overline{X}(t),$$

and the average in time should be zero:

$$E(Y(t)) = 0.$$

A statistical analysis package (described in the next subsection) is applied to $Y(t)$ to determine the sample distribution functions, moments, percentiles, autocorrelation functions, etc. These results are used to select a promising random-process model and to determine the parameters, e.g., a Gauss-Markov process, the variance, and the decorrelation time.

For the random process Z(t), a stochastic simulation of X(t) would be:

$$\hat{X}(t) = \bar{X}(t) + Z(t).$$

Notice that since

$$X(t) = \bar{X}(t) + Y(t),$$

the statistical properties of X and $\hat{X}$ will agree to the extent that those of Z and Y agree.

The rationale for this parameter selection is based on the fact that in typical engagement-model analyses the mean and other statistics of the time series to be simulated are estimated from measured data or acoustic models.

H.2.1.2 Transmission loss

In some applications, the transmission loss fluctuations themselves are simulated as random processes prior to the calculation of the signal time series. In this study, the dominant mechanism for fluctuation in time is assumed to be the movement of the source through static interference patterns. Hence, it is consistent to model the TL fluctuations in range (vice time) at the outset, and then to map these fluctuation properties into the time series via the target motion function. The procedure is the same as that given above, except that there is a range series instead of a time series. If TL(r) has "trend" $\overline{TL}(r)$, then the fluctuation series is

$$Y(r) = TL(r) - \overline{TL}(r).$$

For a random process $Z(r)$ based on the properties of Y, the simulated TL is

$$\hat{TL}(r) = \overline{TL}(r) + Z(r).$$

Now, for a given target with range r(t) and source level SL(t), the signal (before array beamforming or averaging) is

$$S(t) = SL(t) - TL(r(t)) = SL(t) - \{\overline{TL}(r(t)) + Y(r(t))\}$$

The simulated signal is then

$$\hat{S}(t) = SL(t) - \{\overline{TL}(r(t)) + Z(r(t))\}.$$

H.2.2 Some Random-Process Models Used in This Study

Four random-process simulations which have been coded for this study are described next. See Appendix E for the statistical properties of each process.

H.2.2.1 Ehrenfest process

Replications are generated from

$$\tilde{Z}(t) = \frac{i(t) - n/2}{\sqrt{n/4}}$$

at discrete time steps $0,\Delta t,2\Delta t,\ldots,N\Delta t$, where $\Delta t = -\ln(1-2/n)$ and n is the number of "states." For a given initial time, say t=0, i(0) is drawn from a binominal distribution

$$P(i(0)=k) = \binom{n}{k}\left(\tfrac{1}{2}\right)^n,\ k=0,1,\ldots,n.$$

Then i is calculated recursively at steps $k\Delta t$ from

$$i(t+ t) = i(t) + \begin{cases} 1 \text{ if } Y \geq i(t)/n \\ -1 \text{ if } Y \leq i(t)/n \end{cases}$$

where Y is a uniform variable in [0,1], selected at each step.

The zero-mean fluctuation process Z(t) with variance σ^2 and relaxation time τ is found at the discrete time point $k\cdot\Delta t\cdot\tau$ by

$$Z(k\Delta t\tau) = Z(k\Delta t)\cdot\sigma.$$

H.2.2.2 Gauss-Markov process

Begin with an initial sample $\tilde{Z}(0)$ from a normal distribution with $(\mu,\sigma) = (0,1)$, and then calculate recursively

$$\tilde{Z}(t + \Delta t) = \tilde{Z}(t)\cdot e^{-\Delta t} + y\sigma_0$$

where y is a random sample from a normal variable with mean 0 and variance 1, and

$$\sigma_0 = (1 - e^{-2\Delta T})^{1/2}.$$

Then

$$Z(k \cdot \Delta t \cdot \tau) = \tilde{Z}(k\Delta t) \cdot \sigma, \qquad k=0,1,\ldots$$

is a Gauss-Markov realization at discrete time points, with relaxation time τ, variance σ^2, and mean 0.

H.2.2.3 Jump process

The Jump process yields sample paths which are piecewise constant between random "jump" times. Its marginal (1-dimensional) distribution is selectable. A realization from the process is formed as follows:

(1) Select an initial value Z(0), from the Marginal distribution.

(2) Sample n independent values $t_1, t_2, \ldots, t_n$ from a Poisson-distributed variable with parameter $1/\tau$

(3) Sample n independent values from the Marginal distribution: $y_1, y_2, \ldots, y_n$

(4) Set

$$Z(t) = \begin{cases} Z(0) & \text{for} \quad 0 \le t < t_1 \\ y_1 & \text{for} \quad t_1 \le t < t_2 \\ y_2 & \text{for} \quad t_2 \le t < t_3 \\ \cdot & \\ \cdot & \\ \cdot & \\ y_n & \text{for} \quad t_n \le t \end{cases}$$

Then Z(t) has relaxation time τ and the correct marginal distribution.

H.2.2.4 Combination Gauss-Markov and Gauss-Jump

Consider next a simple, linear combination of two random processes. In particular, let

$$Z_c(t) = aZ_G(t) + \sqrt{1 - a^2}\, Z_J(t),$$

where Z_G and Z_J are Gauss-Markov and Gauss-Jump processes, respectively. If Z_G and Z_J have the same variance and relaxation time, τ, then Z_c has an exponential autocorrelation function: $e^{-t/\tau}$.

H.3 Analysis Packages

Two points of view are taken in comparing the signal, noise or signal-to-noise ratio (SNR) time series generated by the acoustic and random-process models. First, the properties of the time series themselves (their statistical distributions, autocorrelation functions, spectra, etc.) are of interest. But secondly, the usefulness of the simulations is in the prediction and analysis of sonar performance, usually detection capability. Hence comparisons are made of "detection histories" for the two types of models. Computer packages for performing each of these comparisons have been developed or applied in this study and are described below.

H.3.1 Statistical Analyses of Time Series Data

A general statistical package has been constructed to study array time-series data. It operates on the matrix

$$\{N(\phi_i, f_j, t_k)\}$$

where $\{\phi_i\}$, $\{f_j\}$, and $\{t_k\}$ are interpreted as the discrete beam pattern indices, frequencies, and time steps, respectively. N can be signal or noise or SNR (in dB). The following calculations are performed.

(a) Histograms are constructed and plotted for any range of i, j and k to specified resolution. Likewise, the mean, variance, skewness, kurtosis, and deciles are found (estimated).

(b) For two of the three independent variables fixed:

- The series is plotted
- A "stationarity" test is performed by dividing the series into any number of equal parts and then applying (a) to each part
- The sample autocovariance function is computed and plotted
- The autocorrelation function is estimated
- An FFT is applied to the autocorrelation function to estimate the power spectral density

(c) For one independent variable fixed, the two-dimensional autocorrelation function is estimated and output in matrix form.

(d) For separation (lag) in one variable, ensembling over the second and for the third fixed, the cross-correlation function is found.

(e) For one variable fixed, one separated, and one lagged, the joint density function for the separated variables is estimated. The histogram is found and multivariate moments calculated.

(f) A Lilliefors Test (see, e.g., Ref. H-4) for goodness-of-fit can be applied to the sample histogram to find best Gaussian fit and test at confidence levels of 0.95 and 0.99.

(g) The logarithmic transformation of the Log-Normal, Non-Central Chi-Square, Chi-Square, Rice, and Rayleigh distributions (see Appendix D) are tested against the sample distribution at levels of 0.95 and 0.99 with the Kolmogorov Test for Fit (see Reference H-4). Graphs of the sample and fitted functions are plotted. Parameter selection is based on the median and other percentile points.

(h) A simplified test for ergodicity calculates ensemble statistics in two directions (e.g., in t and then in replicas for f and ϕ fixed) and compares sample distribution functions at the 0.95 and 0.99 levels with the Smirnov Test (Ref. H-4).

Not all options in the package have been used in this study, but most have proved valuable (especially (a), (b), (d), (f), (g), and (h)) and the remainder should be useful for beam-to-beam or buoy-to-buoy correlation problems. Examples of the application and output of the package can be found in Volume I.

H.3.2 Detector Models

A computer package has been designed to model several types of detectors relevant to this study. Input consists of a time series (ordinarily signal-to-noise ratio) plus relevant parameters. The input time series is converted to a time history of detect/no-detect states according to the following algorithms.

(a) Continuous Threshold detector
Given a time series $\{X(t)\}$, a threshold TH, and a time interval T (holding time), score a detection at time t_o if $X(t) \geq TH$ continuously for $t_o - T \leq t \leq t_o$

(b) Union of Continuous Threshold detector
This is a generalization of (a) except

that a sequence of thresholds and associated holding periods $\{TH_i, T_i\}$ comprises the input. Then detection occurs if the signal X(t) has continuously exceeded a given threshold for the associated holding period for any member of the sequence $\{TH_i, T_i\}$.

(c) Intensity Average detector

Given a time series $\{X(t)\}$, a threshold TH, and an averaging time T, construct

$$S(t_0) = \frac{1}{N} \sum_{j=1}^{N} 10^{X(t_j)/10},$$

where the sum extends over all times t_j such that $t_0 - T \leq t_j \leq t_0$. Score a detect at time t_0 if the intensity average ($S(t_0)$) exceeds the threshold (TH).

(d) Union of Intensity Average detector

This generalizes (c). The input consists of a sequence of thresholds and associated averaging intervals $\{TH_i, T_i\}$. A detection occurs at time t_0 if the intensity average over any one of the averaging periods, T_i, exceeds the associated threshold, TH_i.

(e) N Out of M detector

Given a time-history record {X(t)}, a threshold TH, and integers N and M, a detection occurs if X(t) has exceeded TH for at least N out of M time points immediately preceding and including t_0.

Any one of these detector yields a time history of detect/no-detect. Various statistics are then calculated and displayed, including the distribution of detect (holding) times, no-detect times, associated moments, and order statistics. Again, examples can be found in Volume I.

REFERENCES

H-1 Goldman, J., "A Model of Broadband Ambient Noise Fluctuations Due to Shipping" OSTP-31JG, Bell Laboratories (1974)

H-2 Solomon, L. P., A Barnes, and J. Jao, "Discrete Shipping Model," Planning Systems, Inc. Report (1974)

H-3 McCabe, J. and B. Belkin, "A Comparison of Detection Models Used in ASW Operations Analysis," D. H. Wagner, Assoc. Report to ONR (1973)

H-4 Conover, W. J., Practical Nonparametric Statistics, J. Wiley & Sons, New York (1971)

Distribution List

Address	Copies
1. Defense Advanced Research Projects Agency Washington, DC 20301	
(Tactical Technology Office)	1
(Technical Library)	1
2. Assistant Secretary of the Navy (R,E&S) ATTN: Dr. D. Hyde The Pentagon Washington, DC 20350	1
3. Defense Documentation Center Cameron Station Alexandria, VA 22314	2
4. Chief of Naval Operations Department of the Navy Washington, DC 20350	
(OP-987)	1
(OP-955)	1
5. Chief of Naval Material Department of the Navy Washington, DC 20360	
(ASW-13)	1
6. Office of Naval Research 800 N. Quincy Street Arlington, VA 22217	
(Code 431)	2
(Code 222)	1
(Code 102-OS)	1
(Code 486)	1
7. Naval Sea Systems Command Department of the Navy Washington, DC 20360	
(Code 06H2)	1
8. Naval Research Laboratory Washington, DC 20375	
(Code 8100)	2
9. Naval Electronics Systems Command Department of the Navy Washington, DC 20360	
(PME-124-62)	1
(NAVELEX 320)	1

Distribution List (Cont'd)

Address	Copies
10. Center for Naval Analysis 1401 Wilson Boulevard Arlington, VA 22209	1
11. Naval Ocean Systems Center San Diego, CA 92152 ATTN: H. Schenk	1
12. Naval Underwater Systems Center New London Laboratory New London, CT 06329 ATTN: Mr. R. Hasse	1
13. Bolt, Beranek and Newman, Inc. 1701 North Fort Myer Drive Arlington, VA 22209 ATTN: Dr. M. Moll	1
14. Operations Research, Inc. 1400 Spring Street Silver Spring, MD 20910 ATTN: Dr. E. Moses	1
15. Daniel H. Wagner Associates Station Square One Paoli, PA 19301 ATTN: Dr. B. McCabe	1
16. Systems Control, Inc. 1801 Page Mill Road Palo Alto, CA 94304 ATTN: Dr. J. Anton	1
17. Institute for Acoustic Research 615 Southwest Second Avenue Miami, FL 33130 Mr. J.G. Clark (ATTN)	1
18. Naval Ocean Research andDevelopment Activity Code 320 Bay St. Louis, MS 39520	1